

This is the author-created version of the following work:

Van Reenen, D.D., Huizenga, J.M., Smit, C.A., and Roering, C. (2014) *Fluid-rock interaction during high-grade metamorphism: instructive examples from the Southern Marginal Zone of the Limpopo Complex, South Africa*. *Precambrian Research*, 253 pp. 63-80.

Access to this file is available from:

<https://researchonline.jcu.edu.au/34519/>

Please refer to the original source for the final version of this work:

<http://dx.doi.org/10.1016/j.precamres.2014.06.018>

1 Fluid-rock interaction during high-grade metamorphism: instructive examples
2 from the Southern Marginal Zone of the Limpopo Complex, South Africa

3

4 D.D. Van Reenen^a, J.M. Huizenga^{b,c,*}, C.A. Smit^a, C. Roering^a

5

6 ^a *Department of Geology, University of Johannesburg, Auckland Park, Johannesburg 2006, South Africa*

7 ^b *Economic Geology Research Centre (EGRU), College of Science, Technology and Engineering, James Cook
8 University, Townsville, Queensland, 4811, Australia*

9 ^c *Unit for Environmental Sciences and Management, North-West University, Potchefstroom, 2531, South Africa*

10 * Corresponding author. Tel. +61747814597. E-mail address: jan.huizenga@jcu.edu.au (J.M. Huizenga)

11

12 Keywords: brines; CO₂-rich fluid; granulite; metasomatism; retrograde hydration; Southern
13 Marginal Zone of the Limpopo Complex

14

15 ABSTRACT

16 The Southern Marginal Zone of the Limpopo Complex documents strong evidence that CO₂-
17 rich ($X_{\text{CO}_2}^{\text{fluid}} = 0.7-0.9$, $X_{\text{H}_2\text{O}}^{\text{fluid}} = 0.1-0.3$) and brine fluids of greatly reduced water activity
18 interacted with cooling metapelitic granulite during the thrust-controlled emplacement at
19 2.69-2.62 Ga onto the granite-greenstone terrain of the northern Kaapvaal Craton. Interaction
20 of cooling metapelitic granulite with CO₂-rich fluids at $T < 600-630^\circ\text{C}$ and $P < \sim 6$ kbar is
21 recognized by the presence of a regional retrograde Opx-out/Ath-in isograd and an associated
22 zone of retrograde hydrated granulites that occupies ~ 4500 km² of retrogressed crust located
23 in the hanging wall section of the shallow north-dipping Hout River Shear Zone that bounds
24 the Southern Marginal Zone in the south. On the other hand, brine fluids are considered to
25 have triggered the main pulse of anatexis that resulted in production of large volumes of

26 granodioritic-trondhjemitic melts that intruded and started to interact with metapelitic
27 granulite in the deep crust at $T > \sim 900^{\circ}\text{C}$, $P > \sim 7.5$ kbar. Interaction of hot melt with
28 metapelitic granulite continued until final emplacement in the middle crust ($P = \sim 6$ kbar, $T =$
29 $\sim 630^{\circ}\text{C}$). Brine fluids also initiated shear zone-hosted metasomatism of quartzo-feldspathic
30 gneisses at T between ~ 600 and $\sim 900^{\circ}\text{C}$. and amphibolite-facies lode-gold mineralization.
31 Available data implicate devolatilization of underthrust greenstone material as the dominant
32 deep crustal source for infiltrating CO_2 -rich and brine fluids.

33

34 **1. Introduction**

35

36 Interaction of granulite-facies rocks with externally derived fluids remains a contentious
37 issue among metamorphic petrologists (e.g., Rigby and Droop, 2011; Touret and Huizenga,
38 2011, 2012; Yardley, 2013). This is true because most researchers agree that, in most cases,
39 rocks undergoing high-grade metamorphism have a very low permeability and contain only
40 small amounts of metamorphic fluids at near-lithostatic pressures during peak metamorphism
41 (Yardley and Valley, 1997; Yardley, 2009, 2012). When the metamorphic rocks cool, they
42 hardly back react with fluids to form a lower temperature mineral assemblage (retrogression)
43 because fluids produced during prograde metamorphism escape and thus are no longer
44 available.

45 However, in situ geophysical and geochemical studies carried out in active (modern)
46 regional metamorphic terrains have shown that metamorphic fluids are an integral part of the
47 tectonic system (e.g., Koons and Craw, 1991; Wickham et al., 1993; Wannamaker et al.,
48 1997; Koons et al., 1998). Early studies done in the Himalaya, for instance, established the
49 importance of aqueous fluids being driven out during metamorphism of sediments under the
50 Main Central Thrust when overridden by the hot hanging wall of the Tibetan slab (Le Fort et

51 al., 1987). These fluids triggered anatexis in the hanging wall, which resulted in the
52 generation of leucocratic granite, which intruded into the upper levels of the Tibetan slab (Le
53 Fort et al., 1987).

54 Different workers have also provided mineralogical and isotopic evidence for the
55 existence of high time integrated fluid fluxes and fluid flow directions in many thermal
56 aureoles and regional metamorphic belts (Rubenach, 2013). For example, Markl and Bucher
57 (1998) and Gleeson et al. (2003) have documented evidence for amphibolitization of lower
58 crustal granulites through brine influx, while others (Van Reenen, 1986; Ferry and Dipple,
59 1991; Ferry, 1994; Hoernes et al., 1995; Putnis and Austrheim, 2010) described evidence for
60 infiltration-driven regional metamorphism.

61 The reasons why researchers often doubt whether infiltration metasomatism is
62 widespread during regional metamorphism appears to arise from concerns about the
63 availability and source of fluids (e.g., Yardley, 2013). However, recent experimental data
64 (e.g., Newton and Manning, 2010; Aranovich et al., 2013, under review; Safonov et al., under
65 review) clearly show that, regardless of their origin, deep crustal fluids and specifically
66 brines, must be important agents of metasomatism and mass transfer wherever such processes
67 are recognized in the field or hand specimen (e.g., Harlov, 2012).

68 Wet versus dry middle to deep crust furthermore implicates the issue of fluid-absent
69 (dehydration melting) versus fluid-assisted mechanisms of crustal anatexis. Proponents of the
70 fluid-absent origin of granulite (e.g., Rigby and Droop, 2011) argue that granulite (and crustal
71 anatexis) were formed in the mid to deep crust in the absence of a free fluid phase via high
72 temperature metamorphism (dehydration melting/anatexis; e.g., Fyfe, 1973; Thompson, 1983;
73 Clemens and Vielzeuf, 1987; Waters, 1988; Stevens and Clemens, 1993; Yardley and Valley,
74 1997). A strong argument usually used in favour of the fluid-absent model is that important
75 features of granulite facies rocks support a dehydration melting origin, including the high-

76 temperature nature of a number of granulite assemblages as well as the observation that many
77 granulite-facies rocks preserve the protolith O-isotope signature, thus excluding involvement
78 of a pervasive fluid flow in their origin (e.g., Valley, 1986; Vennemann and Smith, 1992).

79 On the other hand, proponents of the fluid-assisted model for granulite formation and
80 for associated anatexis have shown that temperature estimates ($T < 850^{\circ}\text{C}$) obtained by
81 geothermobarometry from numerous “normal” granulite facies rocks are in fact lower than the
82 values required for the onset of fluid-absent dehydration melting (Aranovich et al., 1987,
83 under review; Newton, 1989; Johannes and Holtz, 1991; Newton et al., 1998, under review;
84 Nair and Chacko, 2002; Safonov et al., under review). They ascribe the apparent undisturbed
85 protolith O-isotope signatures of granulite to low fluid/rock ratios (e.g., Hoernes et al., 1995).
86 The fluid-assisted model is also supported by the common occurrence of CO_2 , brine and
87 mixed CO_2 -brine fluid inclusions (e.g., Touret, 2012; Touret and Huizenga, 2011; Aranovich
88 et al., 2013; Newton et al., under review; Safonov et al., under review). Finally, the presences
89 of large volumes of anatectic granitic melt in high-grade metamorphic terrains argue in favour
90 of a mechanism of “water-fluxed melting” (e.g., Sawyer et al., 2011).

91 High-temperature metasomatism involving chemical and mineralogical changes are
92 undisputable features of high-grade shear zones in granulite-facies terrains and indicates that
93 they are sites of focused fluid flow (Skelton et al., 1995; Smit and Van Reenen, 1997;
94 Glassley et al., 2010; Touret and Huizenga, 2012). Archaean lode-gold mineralisation at
95 different P - T conditions in high-grade gneiss terranes is clearly linked to metasomatism of
96 precursor rocks by infiltrating fluids (e.g., Phillips and Groves, 1983; Phillips, 1985; Smith et
97 al., 1984; Van Reenen et al., 1994; Groves et al., 2003). Such fluids involve H_2O - $\text{CO}_2 \pm \text{CH}_4$
98 fluids (e.g., Mikucki, 1998), with a maximum mole CO_2 mole fraction ($X_{\text{CO}_2}^{\text{fluid}}$) of ~ 0.25
99 derived from crystallizing magma at depth, metamorphic devolatilization reactions, or the
100 mantle as is indicated by stable isotope data (Smith, 1986; Golding et al., 1987; Kerrich,

101 1987). These fluids will, depending on their prevailing temperatures and fluid-rock ratios,
102 either metamorphose or metasomatose (and possibly mineralize) the rocks through which they
103 pass (e.g., Le Fort, 1981; Vrolijk, 1987; Sisson et al., 1989; Moore et al., 1987; Hyndman,
104 1988; Hyndman et al., 1989).

105 Given the complexity of the issues involved, it is imperative that strong field evidence
106 in support of regional and local scale fluid-rock interaction should ideally be interpreted
107 within the context of the overall geological evolution of the rocks in which such processes
108 occur (Yardley, 2013; Huizenga et al., 2014; Smit et al., under review). This paper contributes
109 to specific aspects of this contentious issue by providing, for the first time, a comprehensive
110 record compiled from published (Van Reenen, 1986; Van Reenen and Hollister, 1988; Baker
111 et al., 1992; Hoernes and Van Reenen, 1992; Van Reenen et al., 1994; Van Schalkwyk and
112 Van Reenen, 1992; Hoernes et al., 1995; Smit and Van Reenen, 1997; Van Reenen et al.,
113 2011; Huizenga et al., 2014) and unpublished data (Du Toit, 1994; Mokgatla, 1995; Stefan,
114 1996) regarding interaction of low H₂O-activity ($a_{\text{H}_2\text{O}}^{\text{fluid}}$) fluids and cooling granulites in the
115 Southern Marginal Zone of the Limpopo Complex. Although this paper recognizes
116 devolatilization of underthrust greenstone material as the primary source for infiltrating
117 fluids, we will also discuss alternative fluid sources (crystallizing granitic magma, upper
118 mantle) that might have contributed to the overall fluid budget of the SMZ during the thrust-
119 controlled exhumation.

120 Fluids that infiltrate cooling granulites of the Southern Marginal Zone is expressed by a
121 variety of high-temperature fluid-rock interaction phenomena including pervasive
122 retrogression of granulite, anatexis, and shear zone-hosted metasomatism of high-grade rocks
123 including gold mineralization. High-temperature metamorphic and metasomatic phenomena
124 have shown not to be mutually exclusive but are closely linked processes involving CO₂-rich (
125 $X_{\text{CO}_2}^{\text{fluid}} = 0.7-0.9$, $X_{\text{H}_2\text{O}}^{\text{fluid}} = 0.1-0.3$) fluids and brines. Metasomatism in this context is regarded

126 as changes in the bulk chemical composition of non-volatile components (e.g., Putnis and
127 Austrheim, 2010; Yardley, 2013).

128 Finally, this paper is a general introduction to different case studies in the present issue
129 that deal with special aspects of pervasive and channeled fluid-rock interaction in the
130 Southern Marginal Zone (Dubinina and Aranovich, under review; Koizumi et al., under
131 review; Tsunogae and van Reenen, under review; Safonov et al., under review).

132 Devolatilization of underthrust greenstone material as a specific deep crustal fluid source
133 and a tectono-metamorphic model that controlled persistent fluid flow into overriding hot
134 granulite during exhumation, are the focus of a separate paper (Smit et al., under review).

135

136 **2. Tectonic setting of the Southern Marginal Zone and the northern Kaapvaal Craton**

137

138 The high-grade Limpopo Complex in South Africa is a late Archean ENE-WSW
139 trending zone located between the granite-greenstone terrains of the Zimbabwe and Kaapvaal
140 Cratons (Fig. 1). The complex is subdivided into the Northern Marginal Zone, the Central
141 Zone, and the Southern Marginal Zone (e.g., Van Reenen et al. 2011), of which the Northern
142 and Southern Marginal Zones comprise high-grade granitoids and greenstone belt lithologies
143 (inset in Fig. 1) (e.g., Kreissig et al., 2001; Van Reenen et al. 2011). The Northern and
144 Southern Marginal Zone are juxtaposed against the Zimbabwe and Kaapvaal Craton,
145 respectively, as a result of compression-related exhumation during 2.69-2.62 Ga (Van Reenen
146 et al., 2011). The Central Zone is separated from the marginal zones by Paleoproterozoic
147 crustal-scale strike slip shear zones (e.g., Roering et al., 1992b).

148 The origin and critical role that reactive fluids have played in the Southern Marginal
149 Zone (SMZ) can only be appreciated if this process is considered within the context of the
150 geotectonic relationship of the SMZ with the juxtaposed northern Kaapvaal Craton (NKVC)

151 (Fig. 1, 2). Smit et al. (under review) provide a comprehensive overview of the complex
152 shared evolutionary histories of these two disparate juxtaposed terrains, and only pertinent
153 aspects that impact directly on the focus of this paper will be briefly mentioned here.

154 A shallow north-dipping terrain bounding structure named the Hout River Shear Zone
155 (HRSZ) (Fig. 1, 2) separates two distinct geological terrains that, prior to the onset of the
156 Limpopo Orogeny (~2.72 Ga), formed part of the granite-greenstone terrain of the NKVC.
157 The SMZ of the Limpopo Complex (LC) presently occupies the hanging wall section of this
158 major crustal boundary, whereas granite-greenstone belts of the NKVC occupy the footwall
159 section (Fig. 1, 2). These two disparate terrains are typified by different geological
160 characteristics that evolved as a direct result of the superimposed 2.72-2.62 Ga Limpopo
161 Orogeny (see Smit et al., under review, for a detailed discussion). The following discussion
162 mainly focuses on the evolution of the SMZ.

163 The SMZ comprises foliated, banded and migmatitic enderbitic gneisses (locally
164 known as the Baviaanskloof gneiss) that are complexly infolded with mafic-, ultramafic-, and
165 metapelitic granulite and minor granulite facies BIF of the Bandelierkop Formation (Fig. 1).
166 Major-, trace element-, and isotope geochemical data show that the SMZ represents 3.20-2.99
167 Ga old granite-greenstone material similar to that of the NKVC (Kreissig et al., 2000, 2001).
168 This provides irrefutable evidence that the granulite facies rocks exposed in the SMZ
169 represent the high-grade metamorphic equivalents of granite-greenstone lithologies in the
170 adjacent NKVC (Du Toit et al., 1983; Kreissig et al., 2000, 2001).

171 Emplacement of the SMZ onto the NKVC during the exhumation stage of the LC was
172 controlled by 2.68-2.69 Ga shallow SW-verging HRSZ and related system of steep SW-
173 verging deep crustal shear zones within the SMZ (Fig. 1, 2). This is reflected by: (1)
174 Retrograde metamorphism comprising an early decompression-cooling stage (~2.69 Ga)

175 illustrated by the reaction (Perchuk et al., 2000a, Smit et al., 2001) (mineral abbreviations
176 after Whitney and Evans, 2010):

177



179

180 followed by a near-isobaric cooling stage reflected by the reaction (Perchuk et al., 2000a,
181 Smit et al., 2001):

182



184

185 (2) Regional retrograde hydration caused by CO₂-rich fluids (e.g., Van Reenen et al., 2011),
186 which illustrates the final visible stage of cooling; (3) A zone of retrograde hydrated
187 granulites, separated from the granulites by the retrograde Ath-in/Opx-out isograd (from here
188 onwards referred to as retrograde isograd) resulted from this event; (4) Development of a
189 dominant gneissic (D2) fabric that has developed during exhumation. Regional-scale D2 shear
190 zones are associated with exhumation; (5) Localized D2 shear zoned-hosted metasomatism
191 and lode gold mineralization caused by brines.

192 While the SMZ shows only evidence for high-grade retrograde metamorphism, the
193 underthrust Giyani greenstone belt in the footwall of the HRSZ (Fig. 1), on the other hand,
194 provides evidence for prograde metamorphism at ~2.69 Ga (Van Reenen et al., 1987, 1988,
195 2011; De Wit et al., 1992b; McCourt and Van Reenen, 1992; Roering et al., 1992a; Miyano et
196 al., 1992; Perchuk et al., 1996, 2000; Smit et al., under review).

197

198 **3. Different sources for the retrograde fluids**

199

200 Hollister (1992) discussed three possible sources to account for the retrograde fluid that
201 infiltrated the high-grade rocks of the SMZ during thrust-controlled exhumation and
202 established the retrograde isograd and associated hydration zone: (1) The upper mantle, or
203 mantle derived melts that underplate the lower crust; (2) Crystallizing anatectic melts that
204 originated within the SMZ (Vennemann and Smith, 1992; Stevens, 1997); (3) Prograde
205 devolatilization reactions related to emplacement of hot SMZ granulite over cooler low-grade
206 greenstone belt material of the NKVC (Van Reenen and Hollister, 1988).

207 Hoernes et al. (1995), following on the suggestion by Vennemann and Smith (1992) that
208 O-isotope data failed to identify an external fluid source in the SMZ during hydration, pointed
209 out that recognition of the ultimate fluid source based on O-isotope studies alone is
210 complicated by the fact that the first and second fluid sources are clearly magmatic, and that
211 magmatic rocks (greenstone belt material) also would dominate the third source. This follows
212 from the fact that the SMZ comprises the high-grade metamorphic equivalents of typical
213 greenstone belt material (Kreissig et al., 2001), indicating that the O-isotope signature of the
214 fluids derived from underlying greenstone belts should be similar.

215

216 *3.1. Mantle source*

217

218 Speculations on the possible role of mantle fluids in metasomatism are supported by the
219 fact that mantle fluids include brines and CO₂-rich fluids (e.g., Touret and Huizenga, 2011,
220 2012). Direct evidence that mantle derived mantle fluids have infiltrated the SMZ during
221 exhumation may be provided by C-isotopic compositions of CO₂ extracted from magnesite
222 produced by the high-temperature Ol-breakdown reaction $Ol + CO_2 \rightarrow Opx + Mgs$. This
223 reaction produced a second generation of porphyroblastic Opx in former unhydrated
224 ultramafic granulite (Van Schalkwyk and Van Reenen, 1992). Four samples collected at two

225 different localities in the zone of retrograde hydrated granulites show Mgs $\delta^{13}\text{C}$ values
226 varying between -5.5 and -6.0‰ (Van Schalkwyk and Van Reenen, 1992). However, these
227 values do not conclusively point to a mantle source as similar values are found in different
228 rock types (Kerrick, 1989).

229

230 *3.2. Crystallizing granitic melts*

231

232 Vennemann and Smith (1992) and Stevens (1997) have suggested that water-rich
233 fluids resulting from crystallizing granitic melts (internally buffered fluids) were responsible
234 for the hydration of the cooling granulites under closed-system conditions to produce the zone
235 of retrograde hydration (Fig. 1). In this model, the crystallizing fluids may become enriched in
236 CO_2 species as a result of water-graphite interaction in an oxidized environment (Stevens,
237 1997), while water-rich fluids might evolve into brine fluids during hydration of the granulite
238 (e.g., Markl and Bucher, 1998). However, direct evidence that fluids released by crystallizing
239 granitic melt did interact with hot granulite is restricted to crystallization-hydration (back)
240 reactions that are commonly observed features of metapelitic granulite sampled in close
241 proximity to intrusive leucocratic veins and bodies (Van Reenen et al., 1983; Stevens and Van
242 Reenen, 1992; Safonov et al., under review).

243

244 *3.3. Devolatilization of underthrust greenstone belts*

245

246 A large published database comprising field, structural, and petrological data (Van
247 Reenen, 1986; Van Reenen and Hollister, 1988; Van Reenen et al., 1988, 2011; De Wit et al.,
248 1992a,b; McCourt and Van Reenen, 1992; Miyano et al., 1992; Roering et al., 1992a,b; Van
249 Schalkwyk and Van Reenen, 1992; Perchuk et al., 1996, 2000a,b; Passeraub et al., 1999; Smit

250 et al., 2001) supported by geochemical, isotopic (Kreissig et al., 2000, 2001) and geophysical
251 (e.g., De Beer and Stettler, 1992 and references therein) data provide convincing evidence for
252 a tectono-metamorphic scenario that includes the following essential elements. Firstly, the
253 NKVC dips at shallow angles underneath the SMZ at the position of the HRSZ (Fig. 2).
254 Second, greenstone belt material underlies the SMZ for a distance of at least 40 km north of
255 the HRSZ (De Beer and Stettler, 1992). Third, the overriding granulite interacted thermally
256 and dynamically with underthrust greenstone belts at ~2.69 Ga at the position of the HRSZ
257 (Fig. 2, 3) (e.g., Perchuk et al., 1996). Such a tectono-metamorphic scenario is expected to
258 have resulted in the production of large volumes of fluids derived from devolatilization of
259 underthrust greenstone belts that infiltrated the overriding SMZ. Evidence for this process
260 will be presented and discussed in this paper and further elaborated on in a separate paper
261 (Smit et al., under review). The upper mantle as an additional fluid source will not be further
262 discussed because of a lack of evidence. Safonov et al. (under review) discuss evidence for
263 localized high-temperature fluid-rock interaction of per-aluminous metapelitic granulite with
264 low $a_{\text{H}_2\text{O}}^{\text{fluid}}$ fluids released by crystallizing anatectic trondhjemitic melts at the Petronella
265 locality (Fig. 1) in the SMZ.

266

267 **4. Evidence for high-temperature fluid-rock interaction in the SMZ**

268

269 The SMZ is subdivided into a northern granulite zone that is separated from a southern
270 zone of retrograde hydrated granulite by the retrograde isograd (Fig. 1). Evidence that cooling
271 granulites interacted with immiscible CO₂ and brine fluids of greatly reduced $a_{\text{H}_2\text{O}}^{\text{fluid}}$ at $T >$
272 700°C within the granulite zone (without affecting Opx in metapelitic granulite) will first be
273 discussed, followed by a discussion of pervasive retrograde metamorphism of metapelitic
274 granulite that established the retrograde isograd at $T = 600\text{-}630^\circ\text{C}$. Evidence for high-

275 temperature melt-fluid-rock interaction will be concluded with a discussion of shear zone-
276 hosted metasomatism including the formation of Qz vein-hosted lode gold deposits.

277

278 4.1. *P-T evolution of the SMZ*

279

280 The essentials of the tectono-metamorphic evolution of the SMZ that directly impact
281 on fluid-rock interaction can be summarized with reference to relevant structural-
282 metamorphic data (see Smit et al., under review, for a detailed discussion). *P-T* paths (Fig. 3)
283 were constructed for the common Grt-Opx-Crd/Grt-Sil-Crd bearing assemblages in
284 metapelitic rocks that outcrop throughout the granulite domain (Fig. 1) using the net-transfer
285 reactions (1a) and (1b) and Fe-Mg cation exchange reactions (see Perchuk et al., 2000 for
286 mineral compositions and thermodynamic data and Perchuk, 2011 for a detailed explanation
287 of the methodology). The *P-T* paths show that the retrograde evolution of the SMZ can be
288 linked to two successive stages; an early decompression-cooling (DC) stage that was
289 uninterrupted by a near-isobaric cooling (IC) stage. An important observation is
290 that metapelitic granulite sampled in the granulite domain north of the Annaskraal shear zone
291 (Fig. 1, DR45) only documents evidence for a two-stage DC history (Fig. 3) during which
292 rocks that record maximum *P-T* conditions of ~8 kbar and ~850°C, were initially emplaced
293 into the middle crust ($P = \sim 6$ kbar, $T = \sim 720^\circ\text{C}$, Fig. 3). This was followed by the second DC
294 stage that resulted in emplacement into the upper crust (Fig. 3, DR45). In contrast, similar
295 metapelitic mineral assemblages sampled in the much larger granulite domain located south
296 of the Annaskraal Shear Zone (Fig. 1) document evidence for a near IC stage that commenced
297 at mid-crustal level, i.e. corresponding to the gap between successive stages of DC *P-T* paths
298 (Fig. 3). Near IC *P-T* paths ranging from ~6 kbar and ~700°C to 5-5.5 kbar and 570-600°C
299 (Fig. 3, DR19, DV81, DV101) were followed by decompression-cooling to upper crustal

300 levels (Fig. 3). In this scenario, DC P - T paths are linked to the early exhumation stage of the
301 SMZ that ended with emplacement into the middle crust, whereas IC P - T paths reflect the
302 subsequent thrust-controlled emplacement of the SMZ onto the adjacent NKVC along a near-
303 isobaric surface (6-5.5 kbar), i.e. the HRSZ (Fig. 2) (Smit et al., under review).

304

305 *4.2. Evidence for near-peak fluid-rock interaction during granulite-facies metamorphism*

306

307 Fluid inclusions and microscale metasomatic textures suggest that CO₂-rich fluids and
308 brines interacted with hot granulite at peak and near-peak metamorphic conditions. Primary
309 mixed brine-CO₂ fluid inclusions in Opx and in Qz inclusions in Grt, respectively in
310 metapelitic granulite have been described by Van den Berg and Huizenga (2001) and Touret
311 and Huizenga (2011). These inclusions indicate the coexistence of a brine fluid and pure CO₂
312 at the peak of metamorphism in the SMZ (Touret and Huizenga, 2011).

313 Further, post-peak micro-scale high-temperature fluid-rock interaction is suggested by
314 the common presence of metasomatic perthitic Kfs micro-veins between Qz and Grt in
315 metapelitic granulite (Touret and Huizenga, 2011). Orthopyroxene in contact with these Kfs
316 veins does not show alteration indicating that $a_{\text{H}_2\text{O}}^{\text{fluid}}$ of the fluids responsible for these veins
317 was low (Harlov et al., 1998; Harlov, 2012). The widely accepted interpretation is that Kfs
318 micro-veins are due to influx of low $a_{\text{H}_2\text{O}}^{\text{fluid}}$ brines during the initial phases of post-peak
319 metamorphic uplift (e.g., Harlov et al., 2000; Newton and Manning, 2010; Touret and
320 Huizenga, 2012), identical to the situation described for the granulite zone of the SMZ.
321 Thermocalc pseudosections of the Grt-Bt-Opx-Crd-Kfs-Pl-Qz in the NCKFMASH system
322 show that $a_{\text{H}_2\text{O}}^{\text{fluid}}$ is between 0.4 and 0.5 (Koizumi et al., under review) for P - T conditions of 9
323 kbar and 900°C, respectively. This is consistent with $a_{\text{H}_2\text{O}}^{\text{fluid}}$ calculated from the Bt dehydration
324 reaction using revised thermodynamic data (Newton et al., under review), corresponding to

325 $X_{\text{H}_2\text{O}}^{\text{fluid}}$ being between 0.3 and 0.4 for mixed CO₂-H₂O fluids (Aranovich and Newton, 1999).
326 These $X_{\text{H}_2\text{O}}^{\text{fluid}}$ values relate to H₂O volume fractions between ~0.15 and ~0.25 for the highest
327 density CO₂-rich fluid inclusions reported in the SMZ (homogenization temperature of the
328 CO₂ phase is -30°C; Van den Berg and Huizenga, 2001). Generally, H₂O volume fractions
329 below 0.2 are hardly visible in CO₂-rich fluid inclusions (Bakker and Diamond, 2006).

330 Finally, the observation that metapelitic granulite sampled south of the Annaskraal
331 Shear Zone (Fig. 1) are characterized by near-IC *P-T* paths (Fig. 3, DR19, DV81, DV101)
332 strongly suggests that hot rock emplaced at the middle crustal level cooled rapidly while still
333 at a relatively high pressure. The only reasonable mechanism for rapid cooling of hot
334 granulite at mid-crustal level and distant from the juxtaposed NKVC (Fig. 1) is the infiltration
335 of relatively cool fluids derived from underthrust greenstone belts that underlay much of the
336 granulite domain south of the Annaskraal Shear Zone (Fig. 1, 2) (De Beer and Stettler, 1992;
337 Perchuk et al., 1996, 2000a,b; Smit et al., under review). The observation that rocks north of
338 the Annaskraal shear zone show no evidence for near-isobaric cooling *P-T* trajectories is thus
339 in agreement with the fact that the northern granulite domain is far removed from the area that
340 is underlain by greenstone belts (De Beer and Stettler, 1992; Smit et al., under review).

341

342 *4.3. Dehydration melting versus fluid-induced melting*

343

344 The most contentious issue regarding the role of fluids in the evolution of granulite
345 facies terrains relates to fluid-present versus fluid-absent melting mechanisms that might have
346 accompanied high-grade metamorphism (e.g., Stevens and Van Reenen, 1992; Stevens, 1997;
347 Rigby and Droop, 2011; Touret and Huizenga, 2011; Nicoli et al., in press; Belyanin et al., in
348 press). Evidence for anatexis in the SMZ is reflected by: (1) the presence of migmatitic
349 gneisses comprising tonalitic Baviaanskloof gneiss as well as mafic and metapelitic granulite

350 that characterize the entire SMZ (Du Toit et al., 1983). These migmatites are characterized by
351 small volumes (< 10 vol.%) of leucocratic Pl-Qz (\pm perthite/antiperthite) bearing anatectic
352 material that occurs as small lenticels and veins (cm scale) that enhance the high-grade
353 gneissic fabric of the migmatitic gneisses in which they occur (Fig. 4a). (2) Concordant and
354 discordant almost non-foliated granodioritic/trondhjemitic veins and bodies up to 100 meters
355 high and more than a kilometer wide (Fig. 4b-d). These Pl-Qz-perthite/antiperthite
356 (\pm Grt \pm Crd \pm Sil \pm Bt \pm Gph) bearing bodies (Du Toit et al., 1983; Stevens and Van Reenen,
357 1992) intrude the Bandelierkop Formation (Fig. 4c,d) (Du Toit et al., 1983) implying that they
358 are related to a major pulse of anatexis that post-dated the main granulite facies and
359 deformational events.

360 Kreissig et al. (2001) obtained a U/Pb age (2691 ± 7 Ma) for monazite that occurs as
361 inclusions in plagioclase and biotite coexisting with Grt, Crd, and Opx in migmatitic granulite
362 from the Bandelierkop locality (Fig. 4b). They interpreted this date as the age of monazite
363 growth under granulite facies conditions reflecting the “peak” of granulite facies
364 metamorphism in the SMZ (~ 2.69 Ga). The same authors also obtained a U-Pb zircon age of
365 2643 ± 0.3 Ma for the large (meters wide) granodioritic band exposed in the Bandelierkop
366 locality (Fig. 4b) and interpreted this age, which is significantly younger than that of the
367 metapelitic granulite (~ 2.69 Ga) which it intrudes, to indicate decompression melting during
368 exhumation. This interpretation is supported by U-Pb data of monazite from the leucocratic
369 part of a migmatitic granulite that occurs as a xenolith in the Matok Complex that recorded an
370 age of 2663 ± 4 Ma (Kreissig et al., 2001). It should be noted that Stevens and van Reenen
371 (1992) and Stevens (1997) interpreted this granodioritic band (Fig. 4b) as the product of in-
372 situ prograde fluid-absent partial melting due to muscovite and biotite breakdown reactions
373 (see also Nicoli et al., in press).

374 Evidence that Crd-bearing metapelitic granulite at Bandelierkop quarry interacted with
375 aqueous fluids released by the crystallizing anatectic melt is plainly provided by intergrowths
376 of fine-grained Ged and Ky (Fig. 5a) and coarser-grained Bt and Ky that replaces Crd (Van
377 Reenen, 1983; Stevens and Van Reenen, 1992). However, Opx from the same granulite was
378 not unaffected by this process (Fig. 5a), testifying that a low $a_{\text{H}_2\text{O}}^{\text{fluid}}$ fluid was released during
379 crystallization (Safonov et al., under review).

380 Two prime examples of granodiorite/trondhjemite outcrops on Farm Kameelkuil
381 (S23°13'36.80"; E29°49'19.34") next to the Bandelierkop quarry and on Farm Petronella
382 located about 25 km west-southwest of the Bandelierkop quarry (S23°20'42.43";
383 E29°36'42.72") (Fig. 1). The trondhjemite (Fig. 4d) intruded into high-grade migmatitic
384 metapelitic granulite cutting the D2 fabric. The trondhjemite on Farm Petronella contains
385 small and large remnants of partially assimilated migmatitic metapelitic granulite (Fig. 4d)
386 (Safonov et al., under review). Partially assimilated metapelitic material is also preserved as
387 trails of ferro-magnesium minerals such as Bt, Grt, and Crd that mimic the foliation of the
388 enclosing country rock (Fig. 4d). Garnet porphyroblasts within such trails are often rimmed
389 by symplectic Crd and Opx reflecting evidence for decompression reaction (1a). This reaction
390 was used to determine the retrograde P - T path (sample DR45, Fig. 3) (Perchuk et al., 2000a;
391 Smit et al., 2001) during which the main D2 fabric developed (Smit et al., under review).
392 Features related to the interaction of the metapelitic granulite with fluids expelled by
393 crystallizing trondhjemitic magma are identical to those described at the Bandelierkop quarry
394 and is the focus of a separated paper in the present volume (Safonov et al., under review). The
395 trondhjemitic body at the Petronella locality (Fig. 4d) has recently been dated at ~2.67 Ga
396 (Belyanin et al., under review). This age is in agreement with the emplacement of this
397 magmatic body postdating the main ~2.69 Ga D2 fabric-forming event (Kreissig et al., 2001).

398 The composition (granodioritic to trondhjemitic), intrusive relationships, large
399 volumes, and timing of the main pulse of anatexis (2.67-2.64 Ga) relative to the timing of the
400 main D2 fabric-forming (~2.69 Ga) event at the Bandelierkop quarry and Petronella locality
401 clearly require a mechanism of fluid-fluxed decompression melting. Safonov et al. (under
402 review) show that the tonalitic melt at Petronella locality already intruded the host metapelitic
403 granulite (Fig. 4d) at $P > 7.5$ kbar, $T > 900^{\circ}\text{C}$ and continued to interact with the host rock
404 until final emplacement into the middle crust ($P = \sim 6$ kbar, $T = \sim 630^{\circ}\text{C}$). This scenario
405 strongly argues against the hypothesis that these large bodies might represent the products of
406 in-situ fluid-absent partial melting of muscovite and biotite during the prograde stage of
407 metamorphism (Stevens and Van Reenen, 1992; Stevens, 1997; Nicoli et al., in press). A
408 more plausible scenario based on data presented here and also published as separate papers
409 (Aranovich et al., under review; Newton et al., under review; Safonov et al., under review), is
410 that brine-fluxed decompression melting (Sawyer et al., 2011) resulted in emplacement of
411 granodioritic-trondhjemitic magma into rocks of the Bandelierkop Formation during
412 exhumation. Aranovich et al. (under review) in particular argue that the dehydration-melting
413 model of granite genesis has numerous issues: (1) Heat sources for melting large amounts of
414 the lower crust are often inadequate; (2) H_2O available in mica and amphibole for lower crust
415 dehydration melting is restricted; (3) Depletion of large-ion lithophile elements in granulites
416 cannot be explained by dehydration melting. Furthermore, recently obtained O-isotope
417 fractionation data show that the leucocratic band and host granulite exposed at the
418 Bandelierkop locality (Fig. 4b) are not isotopically related to each other and, therefore,
419 excludes the host metapelitic granulite as a source for these veins (Dubinina et al., under
420 review).

421 Three important issues related to the above scenario should be highlighted. Firstly,
422 fluids expelled by crystallizing melts at both the Bandelierkop and Petronella localities

423 reacted with Crd (Fig. 5a) to form Ged and Ky. Orthopyroxene was not affected, which
424 implies that a low $a_{\text{H}_2\text{O}}^{\text{fluid}}$ fluid was involved. Secondly, Ky and not Sil (Van Reenen, 1983;
425 1986; Safonov et al., under review; Koizumi et al., under review) was produced by Crd
426 hydration (Fig. 5a). This indicates that anatexis and the associated crystallization-hydration of
427 Crd could not be related to fluid-absent dehydration melting at peak metamorphic conditions
428 as suggested by several authors (Stevens and Van Reenen, 1992; Stevens, 1997; Nicoli et al.,
429 in press). In that case one would expect a relatively high temperature and, therefore, Sil to be
430 formed rather than Ky. Finally, Crd hydration at Bandelierkop and Petronella localities (Fig.
431 5a) (Safonov et al., under review) are identical to the observed hydration reactions involving
432 Crd north and on the retrograde isograd (Fig. 5b), and occurred at similar P - T conditions (~6
433 kbar, 600-630°C, see next section). This suggests that distinct hydration phenomena linked to
434 the establishment of the retrograde isograd (next section) and the crystallizing granitic melts
435 in the granulite zone were triggered by similar low $a_{\text{H}_2\text{O}}^{\text{fluid}}$ fluids. Moreover, this also explains
436 the observation that O-isotope fractionation data often fail to identify the presence of an
437 externally derived fluid that interacted with the granulites (Vennemann and Smith, 1992;
438 Hoernes and Van Reenen, 1992; Hoernes et al., 1995), because this fluid was produced as a
439 result of devolatilization of underthrust greenstone material, which is identical to the
440 precursor material of the granulite facies rocks in the SMZ (Kreissig et al., 2000; Van den
441 Berg and Huizenga, 2001).

442

443 *4.4. Pervasive fluid-flow: the regional retrograde isograd*

444

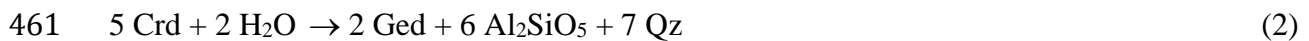
445 *4.4.1. The retrograde isograd*

446

447 An unusual but significant feature of the SMZ is that clear evidence for regional fluid
 448 flow is primarily based on retrograde reactions that occurred at relatively high temperatures
 449 and affected all rock types of the Bandelierkop formation as well as the Baviaanskloof
 450 enderbitic gneiss (e.g., Van Reenen et al., 1983, 2011; Van Reenen, 1986). The infiltrating
 451 fluid rehydrated large areas of the SMZ (> 4500 km²), leaving a sharp demarcation between
 452 unhydrated Opx-Crd-bearing metapelitic granulite in the north (Fig. 6a,b) and hydrated (Opx-
 453 Crd-absent, Ath±Ged±Ky/Sil-bearing gneisses) in the south (Fig. 6c,d) (Fig. 1). This
 454 demarcation is defined by the retrograde isograd that cuts major folds and lithologies in the
 455 central part of the SMZ (Fig. 1) (Van Reenen, 1986), implying that granulite-facies
 456 metamorphism was overprinted by amphibolite-facies metamorphism.

457 Petrographic evidence for regional (pervasive) hydration during cooling is reflected in
 458 metapelitic granulite by two major retrograde hydration reactions involving Opx-Crd-bearing
 459 granulite (Fig. 6c,d) (Van Reenen, 1986; Huizenga et al., 2014):

460



462



464

465 Reaction (2) is not an accurate reflection of the hydration of Crd since Ged does contain up to
 466 2 wt.% Na₂O. This suggests that either a Na-bearing aqueous fluid (Huizenga et al., 2014) or
 467 plagioclase was involved in the reaction. Crd hydration goes hand-in-hand with production of
 468 fine-grained euhedral Grt associated with Ky and Bt. Formation of this assemblage is
 469 probably related to the following reaction (Huizenga et al., 2014):

470



472

473 Reaction (3) defines the retrograde isograd, which can be uninterruptedly mapped from west
474 to east across the entire SMZ (Fig. 1). This reaction resulted in the coexistence of Opx and
475 Ath (Fig. 6c) over a narrow (hundreds of meters) interval in the field (Van Reenen, 1986; Van
476 Reenen et al., 2011) that follows the trend of the HRSZ (Fig. 1). This implies a direct link of
477 pervasive fluid flux with the thrust-controlled exhumation of the SMZ (Fig. 2) (Van Reenen
478 and Hollister, 1988; Van Reenen et al., 2011; Smit et al., under review). Finally, it is
479 important to note that graphite is commonly associated with the products of the reactions (2),
480 (3), and (4) (Van Reenen, 1986; Stevens, 1997).

481

482 *4.4.2. Regional metamorphic control on fluid influx*

483

484 The retrograde isograd has been interpreted to reflect evidence for relatively high-
485 temperature interaction of cooling granulite with an externally derived mobile low $a_{\text{H}_2\text{O}}^{\text{fluid}}$ fluid
486 that infiltrated the overriding high-grade rocks during the thrust controlled exhumation of the
487 SMZ (Fig. 2). Evidence in support of this is outlined below.

488 Orthopyroxene and Ath coexist in metapelitic gneiss along a restricted metamorphic
489 interval (Fig. 1) that separates a granulite zone in the north showing no evidence for Opx
490 hydration (Fig. 6a,b), from a zone of retrograde hydrated granulite in the south where Opx
491 and Crd have been completely replaced by Ath, and Ged and Ky, respectively, as a result of
492 hydration reactions (2) and (3) (Fig. 6c,d) (Van Reenen et al., 1977, 1983, 1986). This
493 observation suggests that hydration reaction (3) should be univariant in the subsystem
494 (Mg,Fe)O₂-SiO₂-H₂O, which is confirmed by the fact that coexisting Opx and Ath have a
495 similar Mg/(Mg+Fe) mole ratio between 0.6-0.7 (Van Reenen, 1986). Moreover, the
496 univariant nature of hydration reaction (3) requires the presence of a free fluid phase that was

497 externally buffered (Van Reenen, 1986). In contrast, the Crd hydration reaction (3) is
498 divariant in the sub-system MgO-FeO-SiO₂-Al₂O₃-H₂O as is shown by contrasting
499 Mg/(Mg+Fe) mole ratios of Crd and Ged (Van Reenen, 1986). Consequently, coexisting
500 reactants and products of reaction (2) straddle the retrograde isograd over a larger surface area
501 in the field. The fact that the retrograde isograd was established as the result of the
502 emplacement of hot granulite over cool greenschist and is superimposed onto major fold
503 structures in the area (Fig. 1) implies a scenario in which regional hydration was controlled by
504 infiltration of a mobile H₂O-bearing fluid (Van Reenen, 1986). If this were not the case,
505 reaction (3) would have been divariant; a scenario that would have resulted in the irregular
506 dispersal of retrograde hydrated granulite closely associated with unhydrated rocks.
507 Systematic variations in the composition of coexisting Grt (Fig. 7a) and Bt (Fig. 7b) in
508 metapelitic granulite compared with their hydrated equivalents indicates that hydration
509 occurred at (near) equilibrium conditions.

510 Mafic and ultramafic gneisses in the hydration zone sometimes still contain partially
511 hydrated high-grade minerals (Van Schalkwyk and Van Reenen, 1992), expressed by relict
512 Cpx and/or Opx, which are being replaced by Hbl and/or Mgs, respectively. The peak
513 assemblage of Fo, Opx, Spl and pargasitic Hbl in ultramafic granulite is replaced by hydrous
514 (Hbl, Chl and Tlc) and carbonate (Mgs, Dol) minerals. This provides conclusive evidence that
515 ultramafic rocks interacted with externally derived CO₂-rich fluid (Van Schalkwyk and Van
516 Reenen, 1992). Moreover, the occurrence of Opx and Cpx relicts in partially hydrated mafic
517 and ultramafic granulite in the hydrated zone of the SMZ (Van Reenen, 1986; De Wit et al.,
518 1992c; Van Reenen et al., 2011) attests to the fact that the granulite occupied the entire SMZ
519 before retrograde hydration occurred (Fig. 1). The general cooling trend is reflected in the Ca-
520 amphibole compositions of the ultramafic rocks (Fig. 7c) (Van Schalkwyk and Van Reenen,
521 1992).

522

523 *4.4.3. P-T constraints and fluid composition*

524

525 Garnet-biotite thermometry, using the calibration by Kaneko and Miyano (2004,
526 2006), of samples on the retrograde isograd (using mineral analyses from Van Reenen, 1986)
527 gave a temperature range of 600-630°C ($P = \sim 6$ kbar) for the breakdown of Opx to Ath
528 (Huizenga et al., 2014). Chemically similar rocks in the zone of hydration (using mineral
529 analyses from Van Reenen, 1986) show slightly lower Grt-Bt temperatures that remain
530 relatively constant at 600-550°C (Huizenga et al., 2014). Pressure conditions on the
531 retrograde isograd are constrained to ~ 6 kbar as Crd hydration on the isograd produced Ky
532 rather than Sil (Van Reenen, 1986; Koizumi et al., under review). However, Sil has been
533 identified as a stable phase in some rocks in the hydrated zone (Van Reenen, 1986). These P -
534 T conditions have been established by numerous other studies (Van Reenen, 1986; Baker et
535 al., 1992; Hoernes et al., 1992; Huizenga et al., 2014; Koizumi et al., under review; Dubinina
536 et al., under review). This suggests that Opx hydration occurred at temperatures more than
537 200°C lower than the temperature ($T = \sim 830^\circ\text{C}$ at $P = \sim 6$ kbar, Fig. 8a) at which En and Ath
538 coexist in presence of a pure H₂O fluid phase (e.g., Newton, 1994; Van Reenen, 1986). A
539 lowering of this equilibrium temperature to 600-630°C is only possible if the hydrating fluid
540 has a $a_{\text{H}_2\text{O}}^{\text{fluid}}$ of 0.2 (Van Reenen, 1986; Van Reenen and Hollister, 1988; Huizenga et al., 2014;
541 Koizumi et al., under review). However, it should be noted that the $a_{\text{H}_2\text{O}}^{\text{fluid}}$ value of 0.2
542 represents a minimum value as Opx and Ath have Mg/(Mg+Fe) mole ratio's between 0.6 and
543 0.7 (Huizenga et al., 2014). Based on the association of graphite with the hydration reactions
544 (2), (3), and (4) (e.g., Huizenga et al., 2014) and other evidence presented below, it can
545 concluded that the low $a_{\text{H}_2\text{O}}^{\text{fluid}}$ fluid phase relates to a CO₂-rich fluid, of which $X_{\text{H}_2\text{O}}^{\text{fluid}}$ ranges
546 between 0.1 and 0.3.

547 Support for a low $a_{\text{H}_2\text{O}}^{\text{fluid}}$ CO₂-rich fluid is, in addition to the presence of graphite, also
548 provided by the partial hydration/ carbonation of ultramafic granulites where the Ol-Ca-Hbl-
549 Opx-Spl peak assemblage has been replaced by a retrograde Ol-Hbl-Opx-Spl-Mgs-Dol-Chl-
550 Tlc assemblage (Fig. 8b) (Van Schalkwyk and Van Reenen, 1992). Of special significance is
551 the replacement of Ol (Van Schalkwyk and Van Reenen, 1992) by Mgs according to the
552 reaction $\text{Ol} + \text{CO}_2 \rightarrow \text{Opx} + \text{Mgs}$, providing evidence that granulite interacted with an
553 externally derived CO₂-rich fluid (Van Schalkwyk and Van Reenen, 1992). The
554 hydrated/carbonated ultramafic assemblage shows that the granoblastic ultramafic rocks were
555 infiltrated at $T = 610\text{-}640^\circ\text{C}$ at $P = 4\text{-}5$ kbar by an externally derived CO₂-rich fluid of which
556 $X_{\text{H}_2\text{O}}^{\text{fluid}} = \sim 0.3$ (Fig. 8b). Note that the pressure should be lower than 6 kbar considering that Sil
557 (produced by Crd hydration) does occur south of the isograd (Van Reenen, 1986).

558 Further evidence for a CO₂-rich fluid is given by fluid inclusion data. Hydrated
559 granulites show dominantly trail bound inclusions composed of (nearly) pure CO₂ (Van
560 Reenen and Hollister, 1988; Touret and Huizenga, 2011; Huizenga et al., 2014). Although
561 H₂O is not visible in the CO₂ inclusions, it has in a few cases been detected by clathrate
562 melting (Van Reenen and Hollister, 1988). This implies that inclusions can contain up to 20
563 vol. % H₂O (corresponding to a maximum $X_{\text{H}_2\text{O}}^{\text{fluid}}$ of 0.3), which is optically undetectable in
564 the inclusions (e.g., Bakker and Diamond, 2006). Considering the P - T conditions of
565 retrograde hydration, CO₂-rich fluid inclusions should have homogenization temperatures
566 (T_h) between -20 and -10°C (Huizenga et al., 2014). However, the lowest T_h that has been
567 found for these inclusions is $+10^\circ\text{C}$. The absence of high-density CO₂-rich fluid inclusions
568 could be explained by re-equilibration during decompression-cooling. However, in that case
569 one would expect a small fraction of the inclusions to maintain their original density (Vityk
570 and Bodnar, 1995; Van den Kerkhof et al., 2014), which is not the case here. Therefore, it is

571 plausible that trapping of the fluid occurred at a pressure between the lithostatic and
572 hydrostatic pressure (Huizenga et al., 2014). Fluid pressures below lithostatic pressures are
573 likely to occur in strike slip shear zones that are present in the hydrated portion of the SMZ
574 (Fig. 1) (Roering et al., 1995). In addition, volume changes associated with hydration
575 reactions (2), (3) and (4) may cause an increase of the rock permeability and, therefore, result
576 in a fluid pressure lower than the lithostatic pressure (Huizenga et al., 2014).

577 Summarizing, retrograde hydration of granulites occurred at $P \leq 6$ kbar and $T \leq 600$ -
578 630°C by means of an infiltrating fluid CO_2 -rich fluid ($0.1 < X_{\text{H}_2\text{O}}^{\text{fluid}} < 0.3$). This is based on (1)
579 volatilization reactions in metapelitic and ultramafic granulites; (2) the presence of graphite in
580 hydrated metapelitic granulites, and (3) the presence of CO_2 -rich fluid inclusions.

581

582 *4.4.4. Open versus closed system behavior during pervasive hydration*

583

584 Whole-rock/mineral O-isotope fractionation patterns (Vennemann and Smith, 1992;
585 Hoernes and Van Reenen, 1992; Hoernes et al., 1995) showed that whereas closed system
586 conditions prevailed in some cases (Fig. 9a), many metapelitic and mafic granulite provided
587 clear evidence for influx of an external fluid and thus open system behavior during pervasive
588 hydration (Fig. 9b,c) (Hoernes et al., 1995). This is demonstrated by whole-rock mineral
589 fractionation patterns for Opx-bearing metapelitic and mafic granulite that show evidence for
590 influx of an externally derived fluid at $T = \sim 635$ - 670°C (Fig. 9a,b). The temperature of
591 1230°C calculated from whole-rock/Opx O-isotope fractionation (Fig. 9b) for the same
592 sample is obviously too high, indicating that closed system behavior is not realistic. The
593 absence of Ath, Ged and Ky from this Opx-Crd-bearing metapelitic granulite implies that
594 hydration started at $T < 670^\circ\text{C}$, i.e. Crd and Opx hydration only occurred when the
595 temperature was low enough (Van Reenen, 1986). Moreover, the temperature of 635°C

596 derived from whole-rock/Ath/Qz O-isotope fractionation (Fig. 9b) is in good agreement with
597 temperature conditions of hydration on the retrograde isograd based on Grt-Bt
598 geothermometry (Van Reenen, 1986; Huizenga et al., 2014).

599 Hoernes and Van Reenen (1992) showed, on the basis of whole-rock/mineral O-
600 isotope data, that the amount of infiltrating fluid necessary to hydrate dry granulite is very
601 small. However, it should be kept in mind that the greenstone belt material in the footwall of
602 the HRSZ is chemically identical to their high-grade equivalents in the SMZ (Kreissig et al.,
603 2001). Fluids derived from the devolatilization of footwall greenstone belts may, therefore, not
604 significantly change the granulite whole-rock/mineral O-isotope system upon infiltration. On
605 the other hand, shear zone-hosted metasomatism in the zone of retrograde hydrated granulite
606 demonstrates isotopic re-equilibration due to focused fluid flow reflecting large fluid-rock
607 ratios (Fig. 9c) (Hoernes et al., 1995).

608

609 *4.4.5. Narrowing of the zone of retrograde hydrated granulite in the western part of the SMZ*

610

611 The dramatic narrowing of the hydration zone in the western part of the SMZ
612 compared with the central part (Fig. 1) is mainly explained by the fact that: (1) the NE-
613 directed dip of the HRSZ changes from near-horizontal in the central part of the SMZ to ~20°
614 in the western part. This change in dip explains the vast exposure of sheared retrograde
615 hydrated gneisses that occur in the hanging wall of the near horizontally north-dipping HRSZ
616 in the central part of the SMZ (Fig. 1, 2). In the area west of the Matok granite (Fig. 1) a much
617 narrower zone of sheared and retrogressed granulite occupies the hanging wall of the much
618 steeper dipping section of the HRSZ (see Smit et al., under review, for a more detailed
619 discussion).

620

621 *4.5. High-temperature metasomatism*

622

623 *4.5.1. Introduction*

624

625 The SMZ offers the opportunity to study high-temperature shear zone-hosted
626 metasomatism. This process includes transformation of (1) dark grey homogenous
627 metamorphic enderbite and banded migmatitic enderbitic gneiss (Baviaanskloof gneiss) into
628 pink Grt-bearing potassium-enriched granite in the granulite zone, (2) banded and
629 retrogressed migmatitic tonalitic gneiss into potassium-enriched granite in the zone of
630 hydrated granulite, and (3) high-temperature shear zone-hosted lode-gold mineralization
631 located both in the footwall and hanging wall sections of the HRSZ. Detailed case studies of
632 shear zone-hosted metasomatic phenomena are the focus of separate papers (Dubinina and
633 Aranovich, under review; Tsunogae and Van Reenen, under review).

634

635 *4.5.2. Shear zone-hosted metasomatic transformation of enderbitic gneiss*

636

637 Excellent continuous outcrops of metasomatically altered and unaltered enderbitic
638 Baviaanskloof gneiss occur within the Petronella Shear Zone on Farms Petronella (Fig. 10a-c)
639 and Commissiedraai (Fig. 10d,e), both located in the granulite zone (Fig. 1). The Petronella
640 locality comprises metapelitic, mafic, and ultramafic granulite, and large volumes of
641 leucocratic anatectic granitoid (Fig. 5d). The locality also provides evidence for numerous
642 local Opx-Pl-Qz-bearing dehydration zones (veins and small bodies) developed within
643 metasomatically altered and unaltered enderbitic gneiss (Fig. 10a) and mafic granulite (Du
644 Toit et al., 1994). Moreover, evidence for hydraulic fracturing under granulite facies
645 conditions is documented by the presence of numerous narrow enderbitic sills that are

646 oriented nearly perpendicular to the principal load (Fig. 10b), and by the presence of
647 granulite-facies breccia (Roering et al., 1995). Roering et al. (1995) interpreted these features
648 as evidence for “deep crustal embrittlement” that resulted from hydro fracturing associated
649 with fluid/melts that infiltrated deep crustal rocks under granulite facies conditions.

650 Grey enderbitic Baviaanskloof gneiss is uninterruptedly altered into a pink
651 metasomatic potassium-enriched granitoid that outcrops continuously over a distance of more
652 than 100 meters in the dry riverbed. The alteration process is easily recognized by the change
653 in color from the unaltered dark grey enderbitic gneiss (Fig. 10a,b) into a pink granitoid
654 characterized by growth of small grains of optically unzoned Mn-rich
655 Grt(\sim Alm₅₄Prp₂₇Sps₁₅Gr₄) (Fig. 10c). Orthopyroxene is preserved in the pink gneiss and
656 seems not to be affected by the alteration process. The metasomatic alteration process
657 involves infiltrating fluids transforming oligoclase in precursor enderbitic gneiss into
658 homogenous ternary K-rich feldspar at temperatures above the ternary feldspar solvus ($T >$
659 \sim 680°C) (Du Toit, 1995). The relatively high temperature of metasomatism is confirmed by
660 Grt-Qz O-isotope fractionation indicating a temperature between 710 and 850°C (Hoernes et
661 al., 1995). Depending on the degree of fluid infiltration, cooling of the homogenous ternary
662 feldspar resulted in antiperthite, mesoperthite or perthite, while microcline is completely
663 absent. Antiperthite typically occurs in the less altered rocks while the more altered rocks are
664 characterized by mesoperthite and perthite (Du Toit, 1995). The isocon diagram (Grant, 1986)
665 shows that metasomatism is accompanied by an increase of K₂O and, to a lesser extent, Na₂O,
666 and a decrease in MgO, FeO, CaO, and TiO₂ (Fig. 11) whereas SiO₂ and Al₂O₃ were
667 immobile (Du Toit, 1994; Smit and Van Reenen, 1997). The alteration process was triggered
668 by a low $a_{\text{H}_2\text{O}}^{\text{fluid}}$ Na-K bearing brine fluid that infiltrated the rock under near-granulite facies
669 conditions to produce a homogenous ternary K-rich feldspar that subsequently exsolved
670 during cooling to produce antiperthite in the less altered, and mesoperthite in the most altered

671 rocks (Du Toit, 1994; Smit and Van Reenen, 1997). The low $a_{\text{H}_2\text{O}}^{\text{fluid}}$ of the metasomatic fluid in
672 the Petronella Shear Zone is supported by the observation that Opx remained stable in narrow
673 metapelitic zones that occur interlayered within metasomatic potassium-enriched granitoid
674 (Du Toit, 1994). Also, the numerous small and near-horizontal oriented Opx-bearing
675 enderbite sills (Fig. 10b) and Opx-Pl-Qz-bearing dehydration zones that occur within the
676 altered rocks show no evidence for interaction with a fluid phase.

677 The Commissiedraai locality shows some differences with the Petronella locality. The
678 precursor enderbite at Commissiedraai is a dark-grey homogenous metamorphic rock (Fig.
679 10d) without any leucocratic veins in contrast to Petronella. Ghost gneissic structures of are
680 preserved within the enderbite and can be traced uninterruptedly into the pink granitoid.
681 Further, alteration is, similar to the Petronella locality, typically characterized by Mn-Grt
682 ($\sim\text{Alm}_{75}\text{Prp}_{15}\text{Sps}_9\text{Gr}_1$) bearing granitoid and narrow foliation zones comprising Sil and Qz
683 (Fig. 10e) whereas microcline is absent (Tsunogae and Van Reenen, under review). Intrusive
684 leucocratic anatectic bodies are absent.

685 Phase equilibrium modeling in the system NCKFMASH using Thermocalc suggested
686 that metasomatic alteration at this locality occurred at $\sim 900^\circ\text{C}$, which corresponds to post-
687 peak metamorphic conditions reached during the initial stage of exhumation in the SMZ
688 (Tsunogae and Van Reenen, under review).

689

690 *4.5.3. Shear zone-hosted metasomatic transformation of hydrated tonalitic gneiss*

691

692 Intense metasomatism of Baviaanskloof gneiss within the retrograde hydrated portion
693 of the SMZ is associated with the D2 Klipbank Shear Zone (locality 3 in Fig. 1). Excellent
694 outcrops in the abandoned dimension stone Klipbank quarry offer the opportunity to study the
695 continuous transformation of precursor retrograde hydrated tonalitic gneiss comprising mainly

696 oligoclase, Bt, Qz and small amounts of Kfs, into intensely altered pink Mn-rich Grt-Sil-
697 bearing potassium-enriched granitoid (Mokgatla, 1995; Smit and Van Reenen, 1997).

698 Potassium metasomatism is characterized by interstitial growth of fine-grained
699 crosshatched microcline at the expense of oligoclase in slightly altered grey-pink gneiss, and
700 by growth of coarse crosshatched microcline replacing oligoclase in most altered pink gneiss.
701 Interstitial microcline in the least altered grey-pink gneiss reflects limited fluid migration
702 along grain boundaries, whereas replacement microcline perthite in the intensely altered pink
703 gneiss suggests the action of a more pervasive K-bearing fluid (Mokgatla, 1995). Mn-rich
704 Alm-Grt ($\sim\text{Alm}_{63}\text{Prp}_{13}\text{Sps}_{24}$) in the highly altered pink gneiss occurs as large zoned
705 porphyroblasts with dark cores due to numerous inclusions mainly of Mag and Ilm. A second
706 generation of small idioblastic Grt crystallized during the retrograde growth stage
707 (Mokgatla, 1995). Similar to Petronella, metasomatism results in an increase of K_2O and
708 Na_2O , and a decrease of MgO , FeO , CaO and TiO_2 whereas SiO_2 and Al_2O_3 remained
709 unchanged (Mokgatla, 1995). The composition of plagioclase varies from $\sim\text{An}_{20}$ in the
710 unaltered rocks to $\sim\text{An}_8$ in the most altered rocks (Mokgatla, 1995).

711 Sillimanite needles in the intensely metasomatized rock are associated with rod-
712 shaped Qz in discrete (mm-wide) shear planes that are oriented parallel to but at high angles
713 relative to the steeply oriented gneissic foliation. Sillimanite needles and Qz rods define a
714 stretching mineral lineation that suggests southwards movement during metasomatism (Smit
715 and Van Reenen, 1997), suggesting a direct link between metasomatism and thrust-controlled
716 exhumation of the SMZ.

717 Complete re-equilibration of intensely altered rocks as the result of interaction with an
718 externally derived fluid is revealed by whole-rock mineral O-isotope fractionation data
719 (Hoernes et al., 1995). The whole-rock/mineral O-isotope fractionation for a metasomatic
720 gneiss from the Klipbank Shear Zone shows that all mineral phases, including Mn-rich Grt,

721 plot reasonably close to a straight line, corresponding to O-isotope equilibration at $T =$
722 $\sim 630^{\circ}\text{C}$ (Fig. 9c, sample KK15, locality 3 in Fig. 1). This temperature is similar to that of the
723 Opx hydration on the isograd, suggesting a direct link with the regional hydration event.
724 Whereas pervasive regional hydration was probably controlled by low CO_2 -rich fluid-rock
725 ratios, shear zone-hosted metasomatism was most likely controlled by a high brine fluid-rock
726 ratio at similar temperature conditions (Huizenga et al., 2014).

727 Summarizing, metasomatism at Klipbank and Petronella involved similar precursor
728 enderbitic/tonalitic gneisses that were transformed into pink Mn-Grt-bearing potassium-
729 enriched granitoid by infiltrating brine fluids. Metasomatic rocks in the Klipbank Shear Zone
730 are characterized by microcline in contrast to those in the Petronella Shear Zone, which show
731 antiperthite, mesoperthite, and perthite. This difference is due to a different temperature of
732 metasomatism: $> 710^{\circ}\text{C}$ along the Petronella Shear Zone and $\sim 630^{\circ}\text{C}$ along the Klipbank
733 Shear Zone (Mokgathla, 1994; Du Toit, 1995; Hoernes et al., 1995; Smit and Van Reenen,
734 1997). Unfortunately, previous studies have mainly focused on the CO_2 rich inclusions in
735 metasomatic rocks in both the Petronella and Klipbank Shear Zones, i.e. a systematic study to
736 identify brine fluid inclusions was not done and will be the subject of a separate study.

737

738 *4.5.4. Shear zone-hosted lode gold mineralization*

739

740 Shear zone-hosted lode gold mineralization has been studied at four localities in the
741 footwall (Giyani greenstone belt in NKVC) (Fig. 1, Birthday, Fumani, Klein Letaba, Frankie),
742 and three localities in the hanging wall (SMZ) (Fig. 1, New Union/Osprey, Louis Moore,
743 Doornhoek) of the HRSZ (Pretorius et al., 1988; Sieber et al., 1991; Van Reenen et al., 1994;
744 Gan and Van Reenen, 1995a,b; Stefan, 1997). The syntectonic ore bodies are located within
745 east west-trending, steeply northward-dipping ductile satellite shear zones of the HRSZ with

746 an oblique to reverse southwest vergence (McCourt and Van Reenen, 1992; Van Reenen et
747 al., 1994). The minimum age obtained from Rb/Sr dating of Ms in pegmatite that intrudes the
748 mineralized shear zones at various localities is ~2.65 Ga (Barton and Van Reenen, 1992). The
749 HRSZ is the first-order control of gold mineralization; more than 90% of known gold deposits
750 in the Giyani greenstone belt (Fig. 1) are situated close to the contact with the HRSZ. The
751 geological characteristics of gold mineralization at these different localities (Table 1) are
752 summarized below.

753 The ore bodies are located within altered mafic (Birthday, Klein Letaba), ultramafic
754 (Louis Moore), and BIF (Fumani, Frankie, Osprey, Doornhoek). Gold occurs either as free
755 milling (inclusions in silicates, e.g. Birthday, Louis Moore) or closely associated with
756 sulphides in syntectonic Qz veins (Table 1).

757 Au mineralizing fluids infiltrated wall-rock at lower- to upper amphibolite facies *P-T*
758 conditions as is indicated by the associated wall-rock alteration (Table 1). Wall-rocks at all
759 deposits are typically enriched in CO₂, K₂O, and S, resulting in extensive Bt and carbonate
760 alteration, which is common to many Archean lode-gold deposits (Table 1) (e.g., Groves et
761 al., 2003). Sulphide mineralization (Apy, Po and Lo) is similar for all deposits despite major
762 differences in wall-rock lithology (Table 1).

763 Structural and metamorphic/metasomatic features that characterize gold mineralization
764 in both the footwall and hanging wall sections of the HRSZ are similar to those of the
765 unmineralized metasomatism in the Klipbank and Petronella Shear Zones. This implies a
766 direct link between the thrust-controlled exhumation of the SMZ in the interval 2.69-2.62 Ga
767 and fluids involved in (1) lode-gold mineralization in both the footwall and hanging wall of
768 the HRSZ, (2) metasomatism in the unmineralized Klipbank and Petronella Shear Zones, and
769 (3) the establishment of the retrograde isograd and associated zone of retrograde hydrated
770 granulite (Van Reenen et al., 1994).

771 Syntectonic gold-bearing Qz veins in all gold deposits typically comprise CO₂-rich
772 (H₂O is not visible, i.e. $X_{\text{H}_2\text{O}}^{\text{fluid}} < 0.2$) and aqueous fluid inclusions of varying salinities,
773 respectively. These inclusions are similar to those documented for granulite and their
774 retrograde hydrated equivalents (Van Reenen and Hollister, 1988; Van Reenen et al., 1994;
775 Van den Berg and Huizenga, 2001), and for the metasomatic enderbitic gneiss at Petronella
776 and Commissiedraai (Du Toit, 1994; Huizenga et al., 2014), and the tonalitic gneiss at
777 Klipbank (Mokgatla, 1995; Huizenga et al., 2014).

778 Summarising, with the present tectono-metamorphic SMZ model in mind, it is likely
779 Au was dissolved from the underlying greenstone belts in brine fluids during prograde
780 metamorphism. The Au-bearing fluid was subsequently focused into the HRSZ and its
781 satellite shear zones. Gold mineralization in the hanging wall of the HRSZ (i.e., retrograde
782 hydrated part of the SMZ: Louis Moore, Osprey/New Union, see Fig. 1) occurred during the
783 regional hydration event. Densities of CO₂-rich inclusions at these localities are relatively low
784 ($T_h > -5^\circ\text{C}$) (Fig. 12a,b). On the other hand, gold mineralization occurred at peak
785 metamorphic conditions in the HRSZ footwall (Birthday, Fumani, Klein Letaba). Densities of
786 CO₂-rich fluid inclusions at these localities are significantly higher (T_h as low as -20°C have
787 been recorded) (Fig. 12c-e).

788

789 **5. Time constraints on fluid infiltration**

790

791 Kreissig et al. (2001) dated the onset of exhumation of the SMZ at ~ 2.69 Ga based on
792 U/Pb monazite data acquired from Grt-Opx-Crd-bearing granulite sampled at the
793 Bandelierkop quarry locality in the SMZ (Fig. 1). In contrast, the peak metamorphic event
794 linked to burial in the root zone of the orogeny has been dated at ~ 2.72 Ga (Retief et al., 1990;
795 Rajesh et al., 2014). SMZ granulites rarely retains evidence for peak metamorphic conditions

796 being reached in the root zone of the orogeny at ~2.72 Ga due to the effect of the
797 superimposed decompression-cooling event (Tsunogae et al., 2004; Belyanin et al., 2012).
798 Therefore, the upper time limit for fluid-flux is constrained by the early stage of exhumation
799 that commenced at ~2.69 Ga, which is supported by the timing (2.68-2.69 Ga) of initial
800 thrusting along the HRSZ (Kreissig et al., 2001; Perchuk et al., 1996, 2000b). The maximum
801 age for the infiltrating fluid is confirmed by the emplacement age of the ~2.68 Ga Matok
802 granitic complex that intrudes the Matok Shear Zone (Laurent et al., 2013) (Fig. 1). Fluid
803 inclusions (Touret and Huizenga, 2011) and whole-rock/mineral O-isotope data (Fig. 4a)
804 (Hoernes et al., 1995) support a scenario in which rocks at granulite grade already interacted
805 with low $a_{\text{H}_2\text{O}}^{\text{fluid}}$ fluids (CO₂-rich and brine fluid) at $T > 800^\circ\text{C}$. The lower time limit for fluid
806 infiltration at $T = 600\text{-}630^\circ\text{C}$, $P = \sim 6$ kbar is constraint by different data. Rb/Sr age data
807 obtained from Ms constrain the time of emplacement of Ms-bearing pegmatite, which intrudes
808 gold-mineralized shear zones at numerous localities along the HRSZ at ~2.65 Ga (Barton and
809 Van Reenen, 1992). On the other hand, Ar³⁹/Ar⁴⁰ age data (2.62-2.63 Ga) (Kreissig et al.,
810 2001) obtained from syn-tectonic Hbl developed in sheared Baviaanskloof gneiss as the result
811 of near isobaric out-of-sequence thrusting associated with the HRSZ, shows that hydration
812 mainly occurred during emplacement of the SMZ onto the Kaapvaal Craton (Van Reenen et
813 al., 2011; Smit et al., under review). Moreover, Belyanin et al. (under review) present new Ar-
814 Ar age data that provide evidence for an extended period of hydration that affected the SMZ
815 during and after its emplacement onto the NKVC.

816

817 **6. Discussions and conclusions**

818

819 Evidence that high-temperature immiscible low $a_{\text{H}_2\text{O}}^{\text{fluid}}$ immiscible CO₂-rich and brine
820 fluids interacted with cooling granulite during the thrust-controlled emplacement of the SMZ

821 of the LC onto the granite-greenstone terrain of the NKVC is sustained by a large dataset.
822 This dataset includes geological-, petrological-, fluid inclusion-, geochemical-,
823 geochronological-, geophysical-, and stable O isotope data.

824 Evidence for pervasive infiltration of high-temperature CO₂-rich fluids is revealed by
825 a regional retrograde (Opx-out/Anth-in) isograd that cuts across major folds and different
826 lithologies. This clearly shows that granulite facies metamorphism in the SMZ was
827 overprinted by a regional amphibolite facies event at $P = \sim 6$ kbar, $T = 600$ - 630°C . Pervasive
828 retrogression established ~ 4500 km² of retrograde hydrated crust that is located in the hanging
829 wall section of the shallow north-dipping shear zone (the HRSZ) that bounds the SMZ in the
830 south. Emplacement of hot granulite over cool granite-greenstone material resulted in
831 devolatilization of the underthrust material that caused large volumes of CO₂-rich and brine
832 fluids to infiltrate hot overriding granulite. This proposed fluid source is strongly supported
833 by geophysical data showing that greenstone belt material at depth presently underlies more
834 than 60% of the SMZ surface area (De Beer and Stettler, 1992; Smit et al., under review).

835 The low $a_{\text{H}_2\text{O}}^{\text{fluid}}$ fluids interacted with rocks in the SMZ at temperature conditions that
836 varied between ~ 600 . and $\sim 900^\circ\text{C}$. This is indicated by: (1) High-temperature metasomatic
837 Kfs micro-veins between Grt and Qz in metapelitic Opx-bearing rocks in the granulite zone;
838 (2) Mixed brine-CO₂ fluid in Opx and in Qz blebs in Grt in metapelitic granulite; (3) Whole-
839 rock/mineral O-isotope fractionation data indicate that granulite interacted with a fluid phase at
840 $T > 800$ - 870°C ; (4) Brine-fluxed partial melting at $T > 900^\circ\text{C}$, $P > 7.5$ - 9 kbar, and (5) Shear
841 zone-hosted metasomatism of quartzo-feldspathic gneiss that occurred at temperatures that
842 ranged from > 710 up to 900°C in the granulite zone to $\sim 600^\circ\text{C}$ within the zone of retrograde
843 hydrated granulite.

844 The relatively low densities of the CO₂-rich fluid inclusions in the retrograde hydrated
845 part of the SMZ suggest that the fluid pressure was below the lithostatic pressure. This can be

846 expected in the SMZ because (Huizenga et al., 2014) it comprises relatively high density of
847 strike slip shear zones, which are characterized by fluid pressures below the lithostatic
848 pressure (e.g., Roering et al., 1995). Further, an increase of rock permeability is also expected
849 due to volume changes associated with the hydration reactions (Huizenga et al., 2014).

850 The main pulse of anatexis resulted in final emplacement of large bodies of anatectic
851 material of granodioritic-trondhjemitic composition at the mid-crustal level into the high-
852 grade gneissic D2 fabric of already migmatitized granulite. This process is explained by a
853 mechanism of brine-induced decompression melting during exhumation. Fluids released by
854 crystalizing granitic melt at mid-crustal level in the granulite zone resulted in hydration
855 reactions involving Crd, Ky, and Ged in the host metapelitic granulite that are identical to
856 regional hydration reactions observed at the retrograde isograd. Finally, near-isobaric cooling
857 reflected by *P-T* paths that commenced at the mid-crustal level during the thrust-controlled
858 emplacement of granulite onto the NKVC, is best explained by the cooling effect of
859 infiltrating fluids.

860

861 **Acknowledgements**

862

863 Numerous MSc and PhD students at the University of Johannesburg (previously the Rand
864 Afrikaans University) have over many years made important contributions to the large
865 database pertaining to the role of fluids in the evolution of the SMZ. Their contributions,
866 largely unpublished, are acknowledged. Different researchers, explicitly Taras Gerya, Lincoln
867 Hollister, Stephan Hoernes, Robert Newton, Leonid Perchuk, and Jacques Touret have
868 significantly contributed to our understanding of the role of fluids in the evolution of high-
869 grade gneiss terrains during many lively discussions in the field at different occasions. Their
870 input is gratefully acknowledged. Informative discussions with conferees during the recent

871 Limpopo Field Workshop in June 2013 are also acknowledged. Their input is gratefully
872 acknowledged. We also would like to thank two anonymous reviewers for their helpful
873 comments and M. Santosh for editorial handling of this paper. DDvR acknowledges financial
874 support over many years from the National Research Foundation of South Africa, as well as
875 continuous support from the Department of Geology and the Faculty of Science at the
876 University of Johannesburg. Financial support of JMH by James Cook University is gratefully
877 acknowledged.

878

879 **References**

880

881 Aranovich, L.Ya., Shmulovich, K.I., Fedkin, V.V., 1987. The H₂O and CO₂ regimes in
882 regional metamorphism. *International Geological Review* 29, 1379-1401.

883 Aranovich, L.Ya., Newton, R.C., 1996. H₂O activity in concentrated NaCl solutions at high
884 pressures and temperatures measured by the brucite-periclase equilibrium. *Contributions
885 to Mineralogy and Petrology* 125, 200-212.

886 Aranovich, L.Y., Newton, R.C., 1999. Experimental determination of CO₂-H₂O activity-
887 composition relations at 600-1000 °C and 6-14 kbar by reversed decarbonation and
888 dehydration reactions. *American Mineralogist* 84, 1319-1332.

889 Aranovich, L.Y., Berman, R.G., 1997. A new garnet-orthopyroxene thermometer based on
890 reversed Al₂O₃ solubility in FeO-Al₂O₃-SiO₂ orthopyroxene. *American Mineralogist* 82,
891 345-353.

892 Aranovich, L.Y., Newton, R.C., Manning, C.E., 2013. Brine-assisted anatexis: experimental
893 melting in the system haplogranite-H₂O-NaCl-KCl at deep-crustal conditions. *Earth and
894 Planetary Science Letters* 374, 111-120.

895 Aranovich, L.Y., Makhlof, A.R., Manning, C.E., Newton, R.C., under review. Dehydration

896 melting and granite-granulite relations. *Precambrian Research*.

897 Baker, J., Van Reenen, D.D., Van Schalkwyk, J.F., Newton, R.C., 1992. Constraints on the
898 composition of fluids involved in retrograde Ath formation in the Limpopo Belt, South
899 Africa. *Precambrian Research* 55, 327-336.

900 Bakker, R.J., Diamond, L.W., 2006. Estimation of volume fractions of liquid and vapor
901 phases in fluid inclusions, and definition of inclusion shapes. *American Mineralogist* 91,
902 635-657.

903 Barton, J.M., Jr., Du Toit, M.C., Van Reenen, D.D., Ryan, B., 1983. Geochronologic studies
904 in the southern marginal zone of the Limpopo mobile belt, southern Africa, in: Van
905 Biljon, W.J., Leg, J.H. (Eds.), *The Limpopo Belt*. Geological Society of South Africa
906 Special Publication 8, pp. 55-64.

907 Barton, J.M., Jr., Doig, R., Smith, C. B., Bohlender, F., Van Reenen, D.D., 1992. Isotopic and
908 REE characteristics of the intrusive charnoenderbite and enderbite geographically
909 associated with the Matok Complex. *Precambrian Research* 55, 451-467.

910 Barton, J.M., Jr., Van Reenen, D.D., 1992a. When was the Limpopo Orogeny? *Precambrian*
911 *Research* 55, 7-16.

912 Belyanin, G.A., Kramers, J.D., Vorster, C., Knoper, M.W., under review. Constraints from
913 ^{40}Ar - ^{39}Ar geochronology on the timing of successive fluid events in the Southern
914 Marginal Zone of the Limpopo Complex, South Africa. *Precambrian Research*

915 Belyanin, G.A., Rajesh, H.M., Sajeev, K., Van Reenen, D.D., 2012. Ultrahigh-temperature
916 metamorphism from an unusual corundum+orthopyroxene intergrowth bearing Al–Mg
917 granulite from the Southern Marginal Zone, Limpopo Complex, South Africa.
918 *Contributions to Mineralogy and Petrology* 164, 457-475.

919 Belyanin, G., Van Reenen, D.D., Safonov, O.G., in press. Reply to the comment on ‘ultrahigh-
920 temperature metamorphism from an unusual corundum-orthopyroxene intergrowth

921 bearing Al-Mg granulite from the Southern Marginal Zone, Limpopo Complex, South
922 Africa by Belyanin et al. (2012)' by Nicoli et al. Contributions to Mineralogy and
923 Petrology.

924 Bohlender, F., Van Reenen, D.D., Barton, J.M., Jr., 1992. Evidence for metamorphic and
925 igneous charnockites in the Southern Marginal Zone of the Limpopo Belt. Precambrian
926 Research 55, 429-449.

927 Brown, M., 2007. Metamorphic conditions in orogenic belts: A record of secular change.
928 International Geology Review 49, 193-234.

929 Clemens, J.D., Vielzeuf, D., 1987. Constraints on melting and magma production in the crust.
930 Earth and Planetary Science Letters 86, 287-306.

931 De Beer, J.H., Stettler, E.H., 1992. The deep structure of the Limpopo Belt. Precambrian
932 Research 55, 173-186.

933 De Wit, M.J. Jones, M.G., Buchanan, D.L., 1992a. The geology and tectonic evolution of the
934 Pietersburg greenstone belt, South Africa, Precambrian Research 55, 123-153.

935 De Wit, M.J., Roering, C., Hart, R.J., Armstrong, R.A., de Ronde, C.E.J., Green, R.W.E.,
936 Tredoux, M., Peberdy, E., Hart, R.A., 1992b. Formation of an Archean continent. Nature
937 357, 553-562.

938 De Wit, M.J., Van Reenen, D.D., Roering, C., 1992c. Geologic observations across a tectono-
939 metamorphic boundary in the Babangu area, Giyani (Sutherland) greenstone belt, South
940 Africa. Precambrian Research 55, 111-122.

941 Du Toit, M.C., Van Reenen, D.D., 1977. The southern margin of the Limpopo Belt, Northern
942 Transvaal, with special reference to metamorphism and structure. Geological Survey of
943 Botswana Bulletin 12, 83-97.

944 Du Toit, M.C., Van Reenen, D.D., Roering, C., 1983. Some aspects of the geology, structure
945 and metamorphism of the Southern Marginal Zone of the Limpopo Metamorphic

946 Complex. in: Van Biljon, W.J., Leg, J.H. (Eds.), The Limpopo Belt. Geological Society
947 of South Africa Special Publication 8, pp. 89-102.

948 Du Toit R., 1994. High temperature metasomatic alteration associated with deep-crustal shear
949 zones in the Limpopo Belt, South Africa. Unpublished M.Sc. thesis Rand Afrikaans
950 University, Johannesburg, 304 pp.

951 Dubinina, E.O., Aranovich, L.Ya, Van Reenen, D.D., Avdeenko, A.S., Kurdyukov, E.B.,
952 Shaposhnikov, V.V., under review. Oxygen isotope systematics of the high-grade rocks
953 of the Southern Marginal Zone of the Limpopo Complex. Precambrian Research.

954 Fyfe, W.S., 1973. The granulite facies, partial melting and the Archean crust. Philosophical
955 Transactions of the Royal Society, London A273, 457-462.

956 Ferry, J.M., Dipple, G.M., 1991. Fluid-flow, mineral reactions, and metasomatism. *Geology*
957 19, 211–214.

958 Ferry, J.M., 1994. Overview of the petrologic record of fluid-flow during regional
959 metamorphism in Northern New-England. *American Journal of Science* 294, 905–988.

960 Ferry J.M., 2007. The role of volatile transport by diffusion and dispersion in driving biotite-
961 forming reactions during regional metamorphism of the Gile Mountain Formation,
962 Vermont. *American Mineralogist* 92, 1288–1302.

963 Gan, S.F., Van Reenen, D.D., 1995a. Geology of gold deposits in the Southern Marginal Zone
964 and the adjacent greenstone belt of the Limpopo Belt; Klein Letaba. *South African*
965 *Journal of Geology* 100, 73-83.

966 Gan, S.F., Van Reenen, D.D., 1995b. Geology of gold deposits in the Southern Marginal
967 Zone and the adjacent greenstone belt of the Limpopo Belt; Franke Mine. *South African*
968 *Journal of Geology*, 98, 263-275.

969 Glassly, W.E., Kortgård, J.A., Sørensen, K., 2010. K-rich brine and chemical modification of
970 the crust during continent-continent collision, Nagssugtoqidian Orogen, West Greenland.
971 Precambrian Research 180, 47-62.

972 Gleeson, S.A., Yardley, B.W.D., Munz, I.A., Boyce, A.J., 2003. Infiltration of basinal fluids
973 into high-grade basement, south Norway: sources and behaviour of waters and brines.
974 Geofluids 3, 33-48.

975 Golding, S.D., Groves, D.I., McNaughton, N.J., Barley, M.E., 1987. Carbon isotope
976 compositions of carbonates from contrasting alteration styles and gold deposits in
977 greenstone belts of the Yilgarn Block and their significance to the source of gold-ore
978 fluids, in: Ho, S.E., Groves, D.I. (Eds.), Recent advances in understanding Precambrian
979 gold deposits. Geology Department and University Extension, University of Western
980 Australia Publications 11, pp. 215-238.

981 Grant, J.A., 1986. The isocon diagram – a simple solution to Gresens' equation for
982 metasomatic alteration. Economic Geology 81, 1976-1982.

983 Groves, D.J., 1993. The crustal continuum model for Late-Archaean lode-gold deposits of the
984 Yilgarn Block, Western Australia, Mineralium Deposita 28, 366-374.

985 Groves, D.I., Goldfarb, R.J., Robert, F., Hart, C.J.R., 2003. Gold deposits in metamorphic
986 belts: overview of current understanding, outstanding problems, future research and
987 exploration significance. Economic Geology 98, 1-29.

988 Harlov, D.E., Hansen, E.C., Bigler, C., 1998. Petrologic evidence for K-feldspar
989 metasomatism in granulite-facies rocks. Chemical Geology 151, 373-386.

990 Harlov, D.E., Wirth, R., 2000. K-feldspar-quartz and K-feldspar-plagioclase phase boundary
991 interactions in garnet-orthopyroxene gneisses from the Val Strona di Omegna, Ivrea-
992 Verbano Zone, northern Italy. Contributions to Mineralogy and Petrology 140, 148-162.

993 Harlov, D.E., 2012. The potential role of fluids during regional granulite facies dehydration in
994 the lower crust. *Geoscience Frontiers*, 1-15.

995 Hoernes, S., Van Reenen, D.D., 1992. The oxygen isotopic composition of granulites and
996 retrogressed granulites from the Limpopo Belt as a monitor of fluid-rock interaction.
997 *Precambrian Research* 55, 353-364.

998 Hoernes, S., Lichtenstein, U., Van Reenen, D.D., Mokgatla, K.P., 1995. Whole rock/mineral
999 O-isotope fractionations as a tool to model fluid-rock interaction. *Precambrian Research*
1000 55, 353-364.

1001 Holdaway, M.J., 1971. Stability of andalusite and the aluminium silicate phase diagram.
1002 *American Journal of Science* 271, 91-131. Holland T.J.B., Powell R., 1998. An
1003 internally consistent thermodynamic data set for phases of petrological interest. *Journal*
1004 *of Metamorphic Geology* 16, 309-343.

1005 Hollister, L.S., 1992. Fluid flow during deep crustal metamorphism, an introduction to new
1006 data from the Southern Marginal Zone of the Limpopo Belt. *Precambrian Research* 55,
1007 321-325

1008 Hyndman, R.D., 1988. Dipping seismic reflectors, electrically conductive zones, and trapped
1009 water in the crust over an subducting plate. *Journal of Geophysical Research* 93, 13391-
1010 13405.

1011 Hyndman, R.D., Shearer, P.M., 1989. Water in the lower continental crust: modeling magneto
1012 telluric and seismic reflection results. *Geophysical Journal International* 98, 343-365.

1013 Johannes, W., Holtz, F., 1991. Formation and ascent of granitic magmas. *Geologische*
1014 *Rundschau* 80, 225-231.

1015 Huizenga, J.M., Van Reenen, D.D., Touret, J.LR., 2014. Fluid-rock interaction in retrograde
1016 granulites of the Southern Marginal Zone, Limpopo high grade terrain, South Africa.
1017 *Geoscience Frontiers*, <http://dx.doi.org/10.1016/j.gsf.2014.01.004>.

1018 Kaneko, Y., Miyano, T., 2004. Recalibration of mutually consistent garnet-biotite and garnet-
1019 cordierite geothermometers. *Lithos* 73, 255-269.

1020 Kaneko, Y., Miyano, T., 2006. Erratum to “Recalibration of mutually consistent garnet-biotite
1021 and garnet-cordierite geothermometers” [*Lithos* 73 (2004) 255–269]. *Lithos* 86, 347.

1022 Kerrich, R., 1987. The stable isotope geochemistry of Au-Ag vein deposits in metamorphic
1023 rocks, in: Kyser, T.K. (Ed.), *Stable isotope geochemistry of low temperature fluids*.
1024 Mineralogical Association of Canada Short Course Handbook 13, pp. 287-336.

1025 Kerrich, R.K., 1989. Archaean gold: Relation to granulite formation or felsic intrusion?
1026 *Geology* 17, 1011-1015.

1027 Kerrich, R., 1998. Geodynamic setting and hydraulic regimes: shear zone-hosted mesothermal
1028 gold deposits, in: Bursnall, J.T. (Ed.), *Mineralization and shear zones*. Geological
1029 Association of Canada Short Course Notes 6, pp. 89-128.

1030 Koizumi, T., Tsunogae, T., Van Reenen, D.D., under review. Fluid evolution of partially
1031 retrogressed polydeformed granulite from the Southern Marginal Zone of the Neoproterozoic
1032 Limpopo Complex, South Africa: evidence from phase equilibrium modelling.
1033 *Precambrian Research*.

1034 Koons, P.O., Craw, D., 1991. Evolution of fluid driving forces and composition within
1035 collisional orogens. *Geophysical Research Letters* 280, 935-938.

1036 Koons, P.O., Craw, D., Cox, S., Upton, P., Templeton, A., Chamberlain, C.P., 1998. Fluid
1037 flow during active oblique convergence. a Southern Alps model from mechanical and
1038 geochemical observations. *Geology* 26, 159-162.

1039 Kramers, J.D., McCourt, S., Roering, C., Smit, C.A., Van Reenen, D.D., 2011. Tectonic
1040 models proposed for the Limpopo Complex: Mutual compatibilities and constraints. in:
1041 Van Reenen, D.D., Kramers, J.D., McCourt, S., Perchuk, L.L. (Eds.), *Origin and
1042 evolution of Precambrian high-grade gneiss terranes, with special emphasis on the*

1043 Limpopo Complex of Southern Africa. Geological Society of America Memoir 207, pp.
1044 311-324.

1045 Kreissig, K., Nögler, T.F., Kramers, J.D., Van Reenen, D.D., Smit, C.A., 2000. An isotopic
1046 and geochemical study of the northern Kaapvaal craton and the Southern marginal Zone
1047 of the Limpopo Belt: are they juxtaposed terranes? *Lithos* 50, 1-25.

1048 Kreissig, K., Holzer, L., Frei, I.M., Villa, J.D., Kramers, J.D., Kröner, A., Smit, C.A., Van
1049 Reenen, D.D., 2001. Geochronology of the Hour River Shear Zone and the
1050 metamorphism in the Southern Marginal Zone of the Limpopo belt, Southern Africa.
1051 *Precambrian Research* 109, 145-173.

1052 Laurent, O., Paquette, J.-L., Martin, H., Doucelance, R., Moyen, J.-F., 2013. LA-ICP-MS
1053 dating of zircons from Meso- and Neoproterozoic granitoids of the Pietersburg block (South
1054 Africa): Crustal evolution at the northern margin of the Kaapvaal craton. *Precambrian
1055 Research* 230, 209-226.

1056 Le Fort, P., Cuney, C., Deniel, C., France-Lanord, C., Sheppard, S.M.F., Upreti, B.N., Vidal,
1057 P., 1987. Crustal generation of the Himalayan leucogranites. *Tectonophysics* 134, 39-57.

1058 Markl, G., Bucher, K., 1998. Composition of fluids in the lower crust inferred from
1059 metamorphic salt in lower crustal rocks. *Nature* 391, 781-783.

1060 Mikucki, E.J., 1998. Hydrothermal transport and depositional processes in Archean
1061 lode-gold systems: A review. *Ore geology Reviews* 13, 307-321.

1062 Miyano, T., Ogata, H., Van Reenen D.D., Van Schalkwyk, H.F., Arawaka, Y., 1992. Peak
1063 metamorphic conditions of sapphirine-bearing rocks in the Rhenosterkoppies greenstone
1064 belt, Northern Kaapvaal Craton, South Africa, in: J.E. Clover, J.E., Ho, S.E., (Eds.), *The
1065 Archean Terranes, Processes and Metallogeny* 31A Symposium Volume, Geology
1066 Department (Key Centre), University of Western Australia, Publication Number 27, pp.
1067 73-87.

1068 McCourt, S., Van Reenen, D.D., 1992. Structural geology and tectonic setting of the
1069 Sutherland greenstone belt, Kaapvaal Craton, South Africa. *Precambrian Research* 55,
1070 93-110.

1071 Mokgatla, K.P.B., 1995. Transformation of tonalitic gneiss into potassic garnet-silimanite
1072 gneis in a deep crustal shear zone in the Limpopo Belt. Unpublished M.Sc. thesis Rand
1073 Afrikaans University, Johannesburg, 163 pp.

1074 Moore, J.C., et al. (ODP Leg 110 Scientific Party), 1987. Expulsion of fluids from depth
1075 along a subduction-zone decollement horizon. *Nature* 326, 785-788.

1076 Newton, R.C. 1989. Fluids in metamorphism. *Annual Review of Earth and Planetary Sciences*
1077 17, 385-410.

1078 Newton, R.C., 1994. Simple-system mineral reactions and high-grade metamorphic fluids.
1079 *European Journal of Mineralogy* 7, 861-881.

1080 Newton, R.C., Aranovich, L.Ya., Hansen, E.C., Vandenheuvel, B.A., 1998. Hyper-saline
1081 fluids in Precambrian deep-crustal metamorphism. *Precambrian Research* 91, 41-63.

1082 Newton R.C., Manning, C.E., 2010. Role of saline fluids in deep-crustal and upper-mantle
1083 metasomatism: insights from experimental studies. *Geofluids* 10, 58-72.

1084 Newton, R.C., Tsunogae, T., under review. Incipient charnockite: Characterization at type
1085 localities. *Precambrian Research*.

1086 Newton, R.C., Touret, J.L.R., Aranovich, L.Y., under review. Fluids and H₂O activity at the
1087 onset of granulite facies metamorphism. *Precambrian Research*.

1088 Nair, R., Chacko, T., 2002. Fluid-absent melting of high-grade semi-pelites: P-T constraints
1089 on orthopyroxene and implication for granulite formation. *Journal of Petrology* 43, 2121-
1090 2142.

1091 Nicoli, G., Stevens, G., Buick, I., Moyen, J-F., in press.. A comment on “ultrahigh-
1092 temperature metamorphism from an unusual corundum-orthopyroxene intergrowth

1093 bearing Al-Mg granulite from the Southern Marginal Zone, Limpopo Complex, South
1094 Africa by Belyanin et al. Contributions to Mineralogy and Petrology.

1095 Passeraub, M., Wuest, T., Kreissig, K., Smit, C.A., Kramers, J.D., 1999. Structure,
1096 metamorphism, and geochronology of the Rhenosterkoppies greenstone belt, South
1097 Africa. South African Journal of Geology 102, 323-334.

1098 Perchuk, L.L., 2011. Local mineral equilibria and P-T paths: Fundamental principles and
1099 applications to high-grade metamorphic terranes, in: Van Reenen, D.D., Kramers, J.D.,
1100 McCourt, S., Perchuk, L.L. (Eds.), Origin and evolution of Precambrian high-grade
1101 gneiss terranes, with special emphasis on the Limpopo Complex of Southern Africa.
1102 Geological Society of America Memoir 207, pp. 61-84.

1103 Perchuk, L.L., Gerya, T.V., Van Reenen, D.D., Safanov, O.G., Smit, C.A., 1996. The
1104 Limpopo metamorphic complex, South Africa: 2 Decompression/cooling regimes of
1105 granulites and adjacent rocks of the Kaapvaal Craton. Petrology 4, 571-599.

1106 Perchuk, L.L., Gerya, T.V., Van Reenen, D.D., Krotov, A.V., Safonov, O.G., Smit, C.A.,
1107 Shur, M.Yu. 2000a. Comparative petrology and metamorphic evolution of the Limpopo
1108 (South Africa) and Lapland (Fennoscandia) high-grade terrains. Mineralogy and
1109 Petrology 69, 69-107.

1110 Perchuk, L.L., Gerya, T.V., Van Reenen, D.D., Smit, C.A., Krotov, A.V, 2000b. P-T paths
1111 and tectonic evolution of shear zones separating high-grade terrains from cratons;
1112 examples from Kola Peninsula (Russia) and Limpopo region (South Africa). Mineralogy
1113 and Petrology 69, 109-142.

1114 Percival, J.A., Roering, C., Van Reenen, D.D., Smit, C.A., 1997. Tectonic evolution of
1115 associated greenstone belts and high-grade terranes, in: De Wit, M.J., Ashwal, L.D.
1116 (Eds.), Greenstone belts. Oxford University Press, Oxford, pp. 398-421.

1117 Philips, G.N., Groves, D.I., 1983. The nature of Archaean gold-bearing fluids as deduced
1118 from gold deposits in western Australia. *Journal of the Geological Society of Australia*
1119 30, 25-39.

1120 Philips, G.N., 1985. Interpretation of Big Bell/Hemlo-type gold deposits: precursors,
1121 metamorphism, melting and genetic constraints. *Transactions of the Geological Society*
1122 of South Africa 88, 159-173.

1123 Pretorius, A.I., Van Reenen, D.D., Barton, J.M. Jr., 1988. BIF-hosted gold mineralization
1124 at the Fumani Mine, Sutherland greenstone belt. *South African Journal of Geology* 4,
1125 429-438.

1126 Putnis, A., Austrheim, H., 2010. Fluid-induced processes: metasomatism and metamorphism.
1127 *Geofluids*, 10, 254-269.

1128 Rajesh, H.M., Santosh, M., Wan, Y., Liu, D., Liu, S.J., Belyanin, G.A., 2014. Ultrahigh
1129 temperature granulites and magnesium charnockites: Evidence for Neoproterozoic accretion
1130 along the northern margin of the Kaapvaal Craton. *Precambrian Research* 246, 150-159.

1131 Rigby, M.J., Droop, G.T.R., 2011. Fluid-absent versus CO₂ streaming during the formation of
1132 polydeformed granulites: A review of insights from the cordierite fluid monitor, in: Van Reenen,
1133 D.D., Kramers, J.D., McCourt, S., Perchuk, L.L. (Eds.), *Origin and evolution of*
1134 *Precambrian high-grade gneiss terranes, with special emphasis on the Limpopo Complex*
1135 *of Southern Africa. Geological Society of America Memoir* 207, pp. 39-60.

1136 Retief, E.A., Compston, W., Armstrong, R.A., Williams, I.S., 1990. Characteristics and
1137 preliminary U-Pb ages of zircon from Limpopo Belt lithologies. *Extended Abstracts, the*
1138 *Limpopo Belt. A field workshop on granulites and deep crustal tectonics, June 21 to July*
1139 *1, 1990. Rand Afrikaans University (now University of Johannesburg).*

1140 Roering, C., Van Reenen, D.D., De Wit, M.J., Smit, C.A. De Beer, J.H., Van Schalkwyk, J.F.,
1141 1992a, Structural geological and metamorphic significance of the Kaapvaal
1142 Craton/Limpopo Belt contact. *Precambrian Research* 55, 69-80.

1143 Roering, C., Van Reenen, D.D., Smit, C.A., Barton, J.M., Jr., De Beer, J.H., De Wit, M.J.,
1144 Stettler, E.H., Van Schalkwyk, J.F., Stevens, G., Pretorius, S., 1992b. Tectonic model for
1145 the evolution of the Limpopo Belt. *Precambrian Research* 55, 539-552.

1146 Roering, C., Van Reenen, D.D., Smit, C.A., Du Toit, R., 1995. Deep crustal embrittlement
1147 and fluid flow during granulite metamorphism in the Limpopo Belt, South Africa.
1148 *Journal of Geology* 103, 673-686.

1149 Safonov, O.G., Tatarinova, D.S., Golunova, M.A., Van Reenen, D.D., Yapaskurt, V.O., under
1150 review. Fluid-assisted interaction of peraluminous metapelites with tonalitic magma in
1151 the Southern Marginal Zone of the Limpopo Complex, South Africa. *Precambrian*
1152 *Research*.

1153 Sawyer, E.W., Cesare, B., Brown, M, 2011. When the continental crust melts. *Elements* 7,
1154 229-234.

1155 Skelton A.D.L., Graham C.M., Bickle, M.J., 1995. Lithological and structural controls on
1156 regional 3-D fluid flow patterns during greenschist-facies metamorphism of the Dalradian
1157 of the SW Scottish Highlands. *Journal of Petrology* 36, 563-586.

1158 Sieber, T., Van Reenen, D.D., Barton, J.M. Jr., 1991. Hydrothermal alteration in the
1159 Matok Complex, Southern Marginal Zone of the Limpopo belt, South Africa, with
1160 implications for gold mineralization. *South African Journal of Geology* 94, 355-364.

1161 Sisson, V.B., Hollister, L.S., Onstott, T.C., 1989. Petrologic and age constraints on the origin
1162 of a low-pressure/high-temperature metamorphic complex, southern Alaska. *Journal of*
1163 *Geophysical Research* 94, 4392-4410.

1164 Smit, C.A., Van Reenen, D.D., 1997. Deep crustal shear zones high-grade tectonites and
1165 associated alteration in the Limpopo belt, South Africa: implication for deep crustal
1166 processes. *Journal of Geology* 105, 37-57.

1167 Smit, C.A., Van Reenen, D.D., Gerya, T.V., Perchuk, L.L., 2001. *P-T* conditions of
1168 decompression of the Limpopo high-grade terrain: record from shear zones. *Journal of*
1169 *Metamorphic Geology* 19, 249-268.

1170 Smit, C.A., Van Reenen, D.D., Roering, C., under review. Fluid-controlled mechanism for
1171 persistent infiltration of overpressured fluids into the Southern Marginal Zone of the
1172 Limpopo Complex, South Africa. *Precambrian Research*.

1173 Smith, T.J., Cloke, P.L., Kesler, S.E., 1984. Geochemistry of fluid inclusions from the
1174 McIntyre-Hollinger gold deposit, Timmins, Ontario, Canada. *Economic Geology* 79,
1175 1265-1285.

1176 Smith, H.S., 1986. Evidence from ^{13}C and ^{18}C isotopes in carbonate minerals for the origin of
1177 fluids in Archaean greenstone belt metamorphic and mineralization processes.
1178 *Geocongress'86, Johannesburg, Extended Abstract Volume*, 341-344.

1179 Stefan, L.S., 1997. Metamorphic and tectonic aspects of the transition from the high-grade
1180 Limpopo Belt to the adjacent low-grade granite-greenstone terrain with special emphasis
1181 on the Doornhoek gold prospect. Unpublished Ph.D thesis Rand Afrikaans University.
1182 pp. 342.

1183 Stevens, G., Van Reenen, D.D., 1992. Partial melting and the origin of metapelitic granulites
1184 in the Southern Marginal Zone of the Limpopo Belt, South Africa. *Precambrian Research*
1185 55, 303-319.

1186 Stevens, G., Clemens, J.D., 1993. Fluid-absent melting and the role of fluids in the
1187 lithosphere: a slanted summary? *Chemical Geology* 108, 1-17

1188 Stevens, G., 1997. Melting carbonic fluids and water recycling in the deep crust, an example
1189 from the Limpopo Belt, South Africa. *Journal of Metamorphic Geology*, 15 141-154.

1190 Thompson, A.B., 1983. Fluid-absent metamorphism. *Journal of the Geological Society of*
1191 *London* 140, 533-547.

1192 Touret, J.L.R., Huizenga, J.M., 2011. Fluids in granulites, in: Van Reenen, D.D., Kramers,
1193 J.D., McCourt, S., Perchuk, L.L. (Eds.), *Origin and evolution of Precambrian high-grade*
1194 *gneiss terranes, with special emphasis on the Limpopo Complex of Southern Africa.*
1195 *Geological Society of America Memoir* 207, pp. 25-37.

1196 Touret, J.L.R., Huizenga, J.M., 2012. Fluid-assisted granulite metamorphism: a continental
1197 journey. *Gondwana Research* 21, 224-235.

1198 Tsunogae, T., Miyano, T., Van Reenen, D.D., Smit, C.A., 2004. Ultrahigh-temperature
1199 metamorphism of the southern marginal zone of the Archean Limpopo Belt, South
1200 Africa. *Journal of Mineralogical and Petrological Sciences* 99, 213-224.

1201 Koizumi, T., Tsunogae, T., Van Reenen, D.D., under review. Fluid evolution of retrogressed
1202 pelitic granulite from the Southern Marginal Zone of the Neoproterozoic Limpopo Complex,
1203 South Africa: evidence from phase equilibrium modeling. *Precambrian Research*.

1204 Rubenach, M., 2013. Structural controls of metasomatism on a regional scale, in: Harlov,
1205 D.E., Austrheim, H. (Eds.), *Metasomatism and the chemical transformation of rock.*
1206 *Springer-Verlag Berlin Heidelberg*, pp. 93-140.

1207 Tsunogae, T., Van Reenen, D.D., under review. High- to ultrahigh-temperature metasomatism
1208 related to brine infiltration in the Neoproterozoic Limpopo Complex: Petrology and phase
1209 equilibrium modeling. *Precambrian Research*.

1210 Valley, J.W., 1986. Stable isotope geochemistry of metamorphic rocks, in: Valley, J.W.,
1211 Taylor, H.P. Jr., O'Neil, J.R. (Eds.), *Stable isotopes in high temperature geological*
1212 *processes. Reviews in Mineralogy and Geochemistry* 16, pp. 445-489.

1213 Van den Berg, R., Huizenga, J.M., 2001. Fluids in granulites of the southern marginal zone of
1214 the Limpopo Belt, South Africa. *Contributions to Mineralogy and Petrology* 141, 529-
1215 545.

1216 Van den Kerkhof, A., Kronz, A., Simon, K., 2014. Deciphering fluid inclusions in high-grade
1217 rocks. *Geoscience Frontiers*, <http://dx.doi.org/10.1016/j.gsf.2014.03.005>

1218 Van Reenen, D.D., 1978. Metamorphic studies of granulite and associated high-grade rocks
1219 from the Southern Marginal Zone of the Limpopo Complex in South Africa. Unpublished
1220 Ph.D. thesis, Rand Afrikaans University, Johannesburg, pp. 478.

1221 Van Reenen, D.D., Du Toit, M.C., 1977. Mineral reactions and the timing of metamorphic
1222 events in the Limpopo Metamorphic Complex south of the Soutpansberg. *Bulletin*
1223 *Botswana Geological Survey* 12, 107-128.

1224 Van Reenen, D.D., Du Toit, M.C., 1978. The reaction garnet + quartz = cordierite +
1225 hypersthene in granulites of the Limpopo Complex in Northern Transvaal, in: (Eds.),
1226 Mineralization in Metamorphic Terrains. Geological Society of South Africa Special
1227 Publication 4, pp. 149-177.

1228 Van Reenen, D.D., 1983. Cordierite+garnet+hypersthene+Bt-bearing assemblages as a
1229 function of changing metamorphic conditions in the Southern Marginal Zone of the
1230 Limpopo metamorphic complex, South Africa, in: Van Biljon, W.J., Leg, J.H. (Eds.), *The*
1231 *Limpopo Belt*. Geological Society of South Africa Special Publication 8, pp. 143-167.

1232 Van Reenen, D.D., 1986. Hydration of cordierite and hypersthene and a description of the
1233 retrograde orthoamphibole isograd in the Limpopo Belt, South Africa. *American*
1234 *Mineralogist* 71, 900-915.

1235 Van Reenen, D.D., Barton, J.M. Jr., Roering, C., Smit, C.A., Van Schalkwyk, J.R. 1987. Deep
1236 crustal response to continental collision: the Limpopo Belt of South Africa. *Geology* 15,
1237 11-14.

1238 Van Reenen, D.D., Hollister, L.S., 1988. Fluid inclusions in hydrated granulite facies rocks,
1239 southern marginal zone of the Limpopo Belt, South Africa. *Geochemica et*
1240 *Cosmochemica Acta* 52, 1057-1064.

1241 Van Reenen, D.D., Roering, C., Smit, C.A., Van Schalkwyk, J.F., Barton, J.M., Jr., 1988,
1242 Evolution of the northern high-grade margin of the Kaapvaal craton. South Africa:
1243 *Journal of Geology* 9, 549-560.

1244 Van Reenen, D.D., Pretorius, A.I., Roering, C., 1994. Characterization of fluids associated
1245 with gold mineralisation and with regional high-temperature retrogression of granulites in
1246 the Limpopo Belt, South Africa. *Geochimica et Cosmochimica Acta* 58, 1147-1159.

1247 Van Reenen, D.D., Perchuk, L.D., Roering, C., Boshoff, R., 2011. Thrust exhumation of the
1248 Neoproterozoic ultrahigh-temperature Southern Marginal Zone, Limpopo Complex:
1249 Convergence of decompression-cooling paths in the hanging wall and prograde P-T paths
1250 in the footwall, in: Van Reenen, D.D., Kramers, J.D., McCourt, S., Perchuk, L.L. (Eds.),
1251 Origin and evolution of Precambrian high-grade gneiss terranes, with special emphasis on
1252 the Limpopo Complex of Southern Africa. *Geological Society of America Memoir* 207,
1253 pp. 189-212.

1254 Van Schalkwyk, J.F., Van Reenen, D.D., 1992. High temperature hydration of ultramafic
1255 granulites from the Southern Marginal Zone of the Limpopo Belt by infiltration of CO₂-
1256 rich fluid. *Precambrian Research* 55, 337-352.

1257 Vennemann, T.W., Smith, H.S., 1992. Stable isotope profile across the orthoamphibole
1258 isograd in the Southern Marginal Zone of the Limpopo Belt, South Africa. *Precambrian*
1259 *Research* 55, 365-397.

1260 Vityk, M.O., Bodnar, R.J., 1995. Do fluid inclusions in high-grade metamorphic terranes
1261 preserve peak metamorphic density during retrograde decompression. *American*
1262 *Mineralogist* 80, 641-644.

1263 Vrolijk, P., 1987. Tectonically driven fluid flow in the Kodiak accretionary complex, Alaska.
1264 *Geology* 15, 466-469.

1265 Watson, E.B., Brenan, J.M., 1987. Fluids in the lithosphere 1. Experimentally determined
1266 wetting characteristics of CO₂-H₂O fluids and their implication for fluid transport, host-
1267 rock physical properties and fluid inclusion formation. *Earth and Planetary Science*
1268 *Letters* 85, 497-515.

1269 Waters, D.J., 1988. Partial melting and the formation of granulite facies assemblages in
1270 Namaqualand, South Africa. *Journal of Metamorphic Geology* 6, 387-404.

1271 Whitney, D.L., Evans, B.W., 2010. Abbreviations for names of rock-forming minerals.
1272 *American Mineralogist* 95, 185-187.

1273 Yardley, B.W.D., Valley, J.W., 1997. The petrologic case for a dry lower crust. *Journal of*
1274 *Geophysical Research* 102, 173-185.

1275 Yardley B.W.D., 2009. The role of water in crustal evolution. *Journal of the Geological*
1276 *Society of London* 166, 585–600.

1277 Yardley, B.W.D., 2013. The chemical composition of metasomatic fluids in the crust. in:
1278 Harlov, D.E., Austrheim, H. (Eds.), *Metasomatism and the Chemical Transformation of*
1279 *Rock*, *Lecture Notes in Earth System Sciences*, Springer-Verlag, Berlin, Heidelberg, pp.
1280 16-51.

1281

1282 FIGURE CAPTIONS

1283

1284 Figure 1

1285

1286 Geological map of the SMZ/NKVC contact area that highlights major features: (1) the
1287 shallow southwest-verging terrain-bounding HRSZ and related southwest-verging high-grade
1288 shear zones within the SMZ; (2) opposing tectonic transport directions of rocks at ~2.72 Ga
1289 within the NKVC and at ~2.69 Ga within the SMZ (grey and white arrow, respectively); (3)
1290 the position of the retrograde isograd that subdivides the SMZ into a northern granulite zone
1291 and southern zone of retrograde hydrated granulite located in the hanging wall section of the
1292 HRSZ; (4) ~2.68 Ga granitoid intrusives (Matok) in both the SMZ and NKVC. Localities
1293 referred to in the text: 1-Bandelierkop Quarry, 2-Petronella and Commissiedraai locality
1294 (Petronella Shear Zone), 3-Klipbank locality (Klipbank Shear Zone), 4-Sample locality
1295 DR45, 5- Sample locality DV81, 6- Sample locality DR19, 7- Sample locality DV101, 8-
1296 Sample locality DV400, 9- Sample locality DR191. Gold deposit localities: a-Birthday, b-
1297 Fumani, c-Klein Letaba and Frankie, d-Louis Moore, e-New Union/Osprey, f-Doornhoek. SZ:
1298 shear zone; GB: greenstone belt.

1299

1300 Figure 2

1301

1302 Schematic crustal section (see Fig. 1 for cross section locality) demonstrating the relationship
1303 of the SMZ with the underthrust granite-greenstone terrain of the NKVC (modified after
1304 Roering et al., 1992a, Smit et al., under review). Lines with solid arrow heads indicate general
1305 movement of crustal segments in the SMZ as represented by samples DR45 and DR 19 (see
1306 Fig. 3). HRSZ: Hout River Shear Zone.

1307

1308 Figure 3

1309

1310 (a) P - T - t diagram demonstrating the dynamic and thermal interaction of underthrust
1311 greenschist (black dotted arrow) with overriding granulite. Indicated are the prograde, peak
1312 and initial retrograde P - T loop (grey dotted arrow) (Belyanin et al., 2012; Belyanin et al., in
1313 press), and the composite retrograde P - T paths (solid black arrow). (b) Detailed retrograde P -
1314 T paths (samples DR19, DR45, DV81 and DV101, see Fig. 1 for sample localities) for the
1315 SMZ and P - T loop for underthrust greenschists (Giyani Greenstone Belt) (Perchuk et al.,
1316 2000a). DR45 indicates a DC path reflected by reaction (1a). DR19, DV81, and DV101
1317 record an intervening IC, reflected by reaction (1b) between early and final DC paths.
1318 Geochronological data after Retief et al. (1990), Kreissig et al. (2001) and Belyanin et al.
1319 (under review). The subdivision of the granulite facies into different P - T regimes is after
1320 Brown (2007): HT = high temperature; UHT = ultrahigh temperature; HP = high pressure.
1321 The Al-silicate system is after Holdaway (1971). See text for discussion.

1322

1323 Figure 4

1324

1325 Illustration of successive anatexis events in the SMZ. (a) Small anatexis veins and melt
1326 patches (Petronella locality, Fig. 1) enhance the gneissic fabric of metapelitic granulite. (b)
1327 Concordant veins of granodioritic/trondjhemitic composition developed within metapelitic
1328 granulite at Bandelierkop locality (Fig. 1). The major vein dated at ~2.64 Ga (Kreissig et al.,
1329 2001) intruded the migmatitic metapelitic host rock dated at ~2.69 Ga (Kreissig et al., 2001).
1330 (c) Intrusive relationship of granodioritic body (light-coloured) with metapelitic granulite
1331 (dark-coloured) at Bandelierkop locality. The granodiorite comprises metapelitic xenoliths

1332 (not visible in the photograph) and crosscuts the darker metapelite. A weak gneissic foliation
1333 developed within the leucocratic body suggests emplacement during deformation. (d) Large
1334 body (~1 km in width) of leucocratic trondjhemitic dated at ~2.67 Ga (Belyanin et al., under
1335 review) that intruded and partially assimilated metapelitic granulite (Petronella locality). Note
1336 the presence of a narrow metapelitic xenolith (centre) and of a partially digested metapelitic
1337 xenolith (centre left) defined by Grt-Bt-Crd trails near the country rock.

1338

1339 Figure 5

1340

1341 Plane-polarised light microphotographs demonstrating hydration reactions involving Crd
1342 within the granulite zone. See text for discussion. (a) Localised cordierite hydration at the
1343 Petronella locality (Fig. 1). Cordierite is replaced by fine-grained intergrowths of Ged and Ky,
1344 and by coarser-grained Bt and Ky. Opx remains unaltered. (b) Regional hydration of Crd
1345 north of the retrograde isograd. Here, initial hydration of Crd is shown by its replacement at
1346 the edges by needle-shaped fine-grained Ged and Ky. Note that Opx is stable, confirming the
1347 low $a_{\text{H}_2\text{O}}^{\text{fluid}}$ of the hydrating fluid.

1348

1349 Figure 6

1350

1351 Plane-polarised light microphotographs showing petrographic features of metapelitic granulite
1352 (a, b) and their hydrated equivalent (c, d). See text for discussion. (a) Granoblastic texture of
1353 cordierite-free Grt granulite. (b) Reaction texture preserving evidence for the decompression
1354 cooling reaction $\text{Grt} + \text{Qz} \rightarrow \text{Crd} + \text{Opx}$ (photo from Huizenga et al., 2014). (c) Isograd
1355 reaction (2) developed in Crd-free granulite on the retrograde isograd. (d) Completely
1356 hydrated $\text{Ath} \pm \text{Ged} \pm \text{Ky} \pm \text{Grt}$ gneiss from the hydrated granulite zone.

1357

1358 Figure 7

1359

1360 Changing compositions of (a) Grt and (b) Bt in metapelitic gneiss, and (c) Ca-amphibole in
1361 ultramafic rocks from the granulite zone (open circles), the retrograde isograd (solid black
1362 circles), and retrograde hydrated granulite zone (grey circles). (a) and (b) modified after Van
1363 Reenen (1986), (c) modified after Van Schalkwyk and Van Reenen (1992). Note that no
1364 ultramafic isograd samples were found. Grey arrow indicates the mineral compositional trend
1365 from the granulite to the retrograde hydrated granulite zone.

1366

1367 Figure 8

1368

1369 (a) Composition of the hydrating fluid constrained by P - T conditions of ~6 kbar, 600-630°C
1370 calculated for the retrograde isograd reaction (3) (assuming Mg-end members). The reaction
1371 curve was calculated using Holland and Powell's dataset (1998). (b) Composition of
1372 infiltrating CO₂-rich fluid phase constrained by petrological modeling of partially hydrated
1373 and carbonated ultramafic assemblages in sample DR191 (see Fig. 1 for sample locality).
1374 Reaction curves are calculated using the dataset by Holland and Powell (1998). Mineral
1375 compositions are from Van Schalkwyk and Van Reenen (1992). Activities for the end
1376 members were calculated using the program AX developed by T. Holland. See text for
1377 discussion. For both (a) and (b) $a_{\text{H}_2\text{O}}^{\text{fluid}}$ was recalculated to $X_{\text{H}_2\text{O}}^{\text{fluid}}$ using the H₂O-CO₂ activity-
1378 composition model from Aranovich and Newton (1999).

1379

1380 Figure 9

1381

1382 Fractionation coefficient versus $\delta^{18}\text{O}$ diagrams (FCD diagrams) for (a) metapelitic gneiss
1383 from the hydrated granulite zone (sample P50C in Hoernes et al., 1995), (b) metapelitic gneiss
1384 from the granulite zone (sample P19C in Hoernes et al., 1995), and (c) metasomatized
1385 tonalitic gneiss from the Klipbank Shear Zone (sample KK15 in Hoernes et al., 1995) (see
1386 Fig. 1 for locality) (a) Near-peak T ($\sim 820^\circ\text{C}$) is derived from whole-rock/Grt fractionations.
1387 Whole-rock/Ath fractionation defines a secondary linear array with a flatter slope
1388 corresponding to Ath formation at $T = \sim 635^\circ\text{C}$. (b) Whole-rock/Qz/Pl/Opx fractionation
1389 indicates fluid-induced re-equilibration at $T = \sim 670^\circ\text{C}$. Whole-rock/Grt fractionation gives an
1390 unrealistically high temperature (1230°C) (Hoernes et al., 1995). (c) All phases plot
1391 reasonably close to a straight line, suggesting re-equilibration at $T = 630^\circ\text{C}$ due to fluid
1392 infiltration. Note the close correspondence of this temperature to that of the retrograde
1393 hydration on the isograd. Figure modified after Hoernes et al. (1995).

1394 Figure 10

1395

1396 Shear zone-hosted metasomatism at the Petronella (a-c) and Commissiedraai (d-e) localities
1397 (Fig. 1). (a) General view of strongly foliated altered pink rocks (straight gneisses, Smit and
1398 Van Reenen, 1997) in the Petronella Shear Zone. The precursor grey enderbitic gneiss (dark-
1399 grey bands alternating with pink bands in b) is altered into light-pink metasomatic potassium-
1400 enriched metasomatic rocks (c). (b) Selective metasomatism of leucocratic veins within the
1401 enderbitic gneiss. Note the presence of a narrow near-horizontal enderbitic sill (pen) that
1402 intrudes both the enderbitic gneiss and the metasomatized leucocratic veins. (c) Intensely
1403 altered enderbitic gneiss transformed into pink Mn-rich Grt-bearing potassium-enriched
1404 granitoid. (d) Dark grey homogenous metamorphic enderbite (HE) metasomatized into pink
1405 Grt-Opx-bearing potassium enriched enderbite (ME). Ghost gneissic structures of the
1406 precursor gneiss is preserved within the metamorphic enderbite and can be traced

1407 uninterruptedly into the pink granitoid. (e) Intense metasomatism resulting in Sil-bearing
1408 (Opx absent) sheared granitoid.

1409

1410 Figure 11

1411

1412 Isocon diagram showing gains and losses of major oxides with increasing metasomatic
1413 alteration from the least-altered (open circles) to the most-altered enderbitic (solid circles)
1414 gneiss at Petronella. Assuming constant Al_2O_3 (e.g., Newton and Tsunogae, under review),
1415 volume and mass have not changed during the metasomatic process. TiO_2 , P_2O_5 , CaO , FeO ,
1416 and MgO are lost during metasomatism whereas Na_2O and K_2O are gained. Dotted lines
1417 indicate the relative gains and losses. For example, the relative concentration decrease of
1418 MgO is ~81%. Figure modified after Smit and Van Reenen (1997) using data by Du Toit
1419 (1994).

1420

1421 Figure 12

1422

1423 Bar plots (bar width: $2^\circ C$) of Th for CO_2 -rich fluid inclusions in gold-bearing Qz veins in
1424 shear zone-hosted lode-gold mineralization in the hanging wall (a, b) and footwall (c-e) of the
1425 HRSZ. See Fig. 1 for gold deposit localities. Figure modified after Van Reenen et al. (1994).
1426 See text for discussion.

1427

1428 TABLE CAPTIONS

1429

1430 Table 1.

1431

1432 Characteristics of Au mineralization related to the tectono-metamorphic evolution of the SMZ

1433 using data from Pretorius et al. (1988), Van Reenen et al. (1994), Gan and Van Reenen

1434 (1995a,b), and Stefan (1997). See Fig. 1 for gold deposit localities.

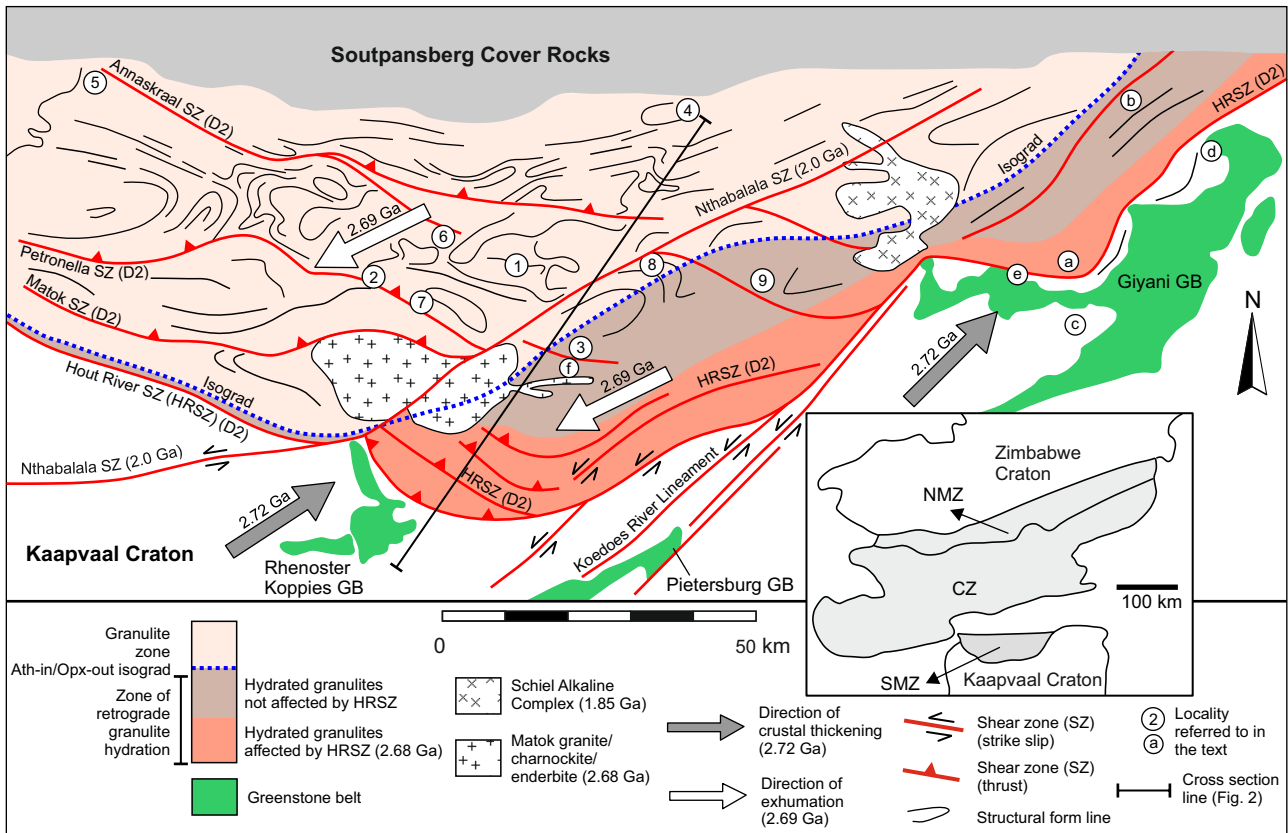


Figure 1 (colour)

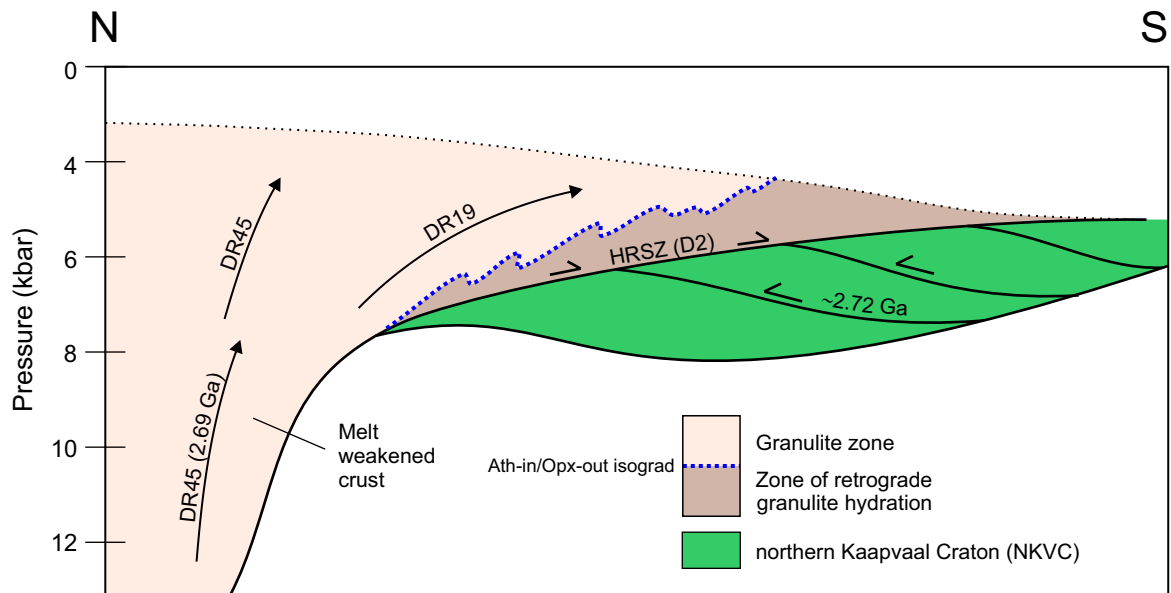


Figure 2 (colour)

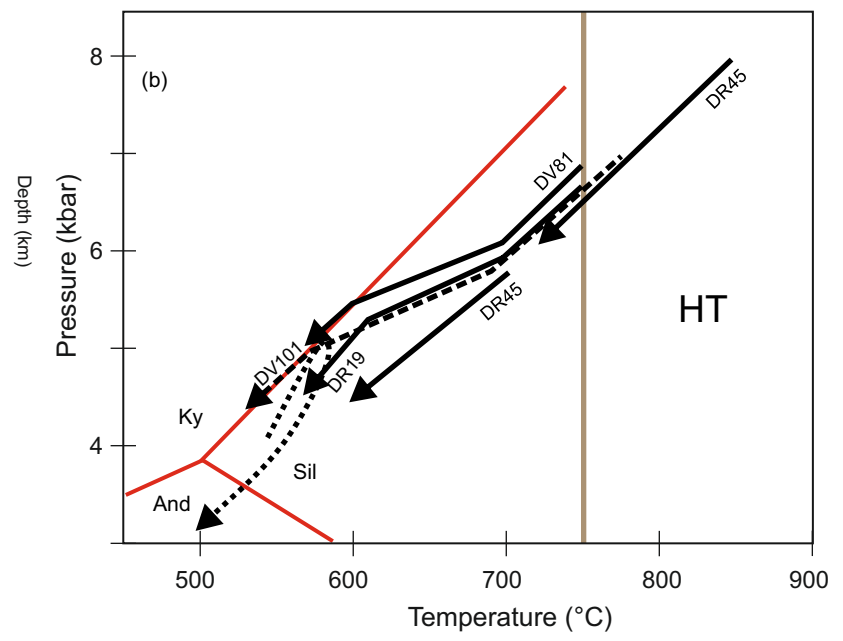
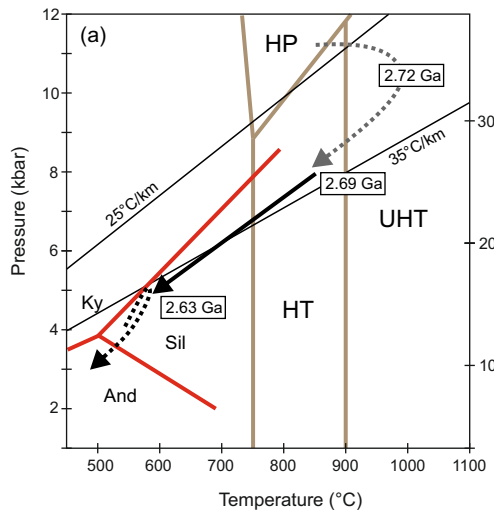


Figure 3 (colour)

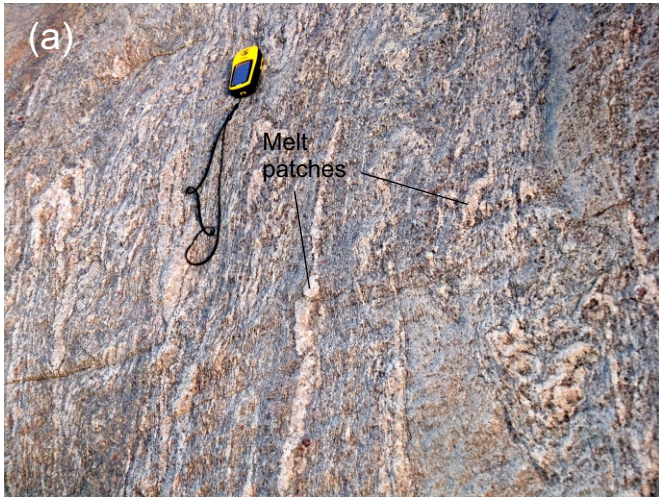
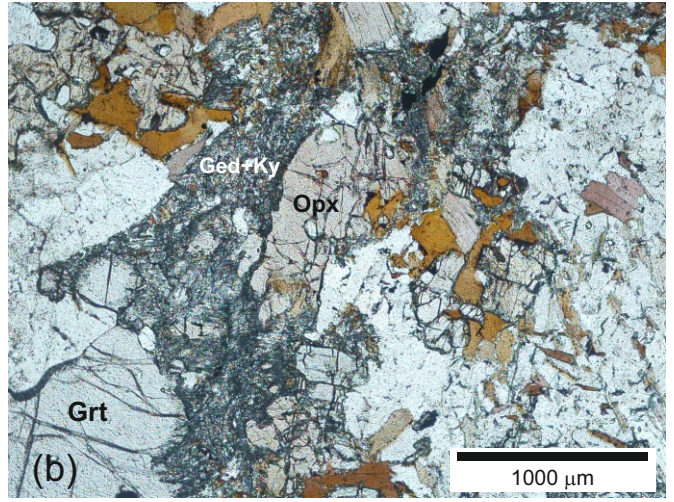
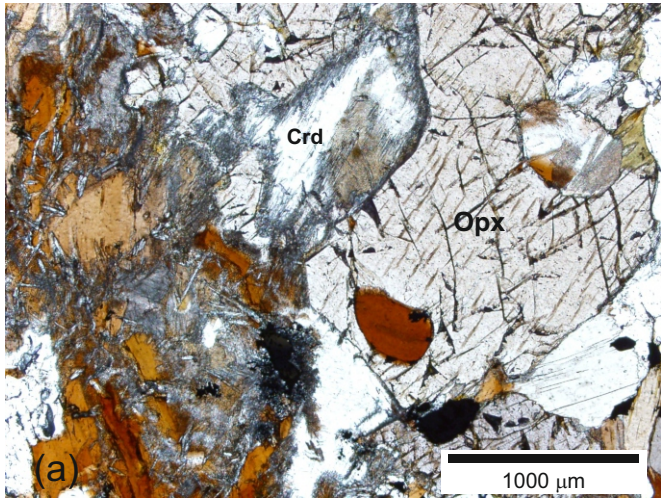


Figure 4 (colour)



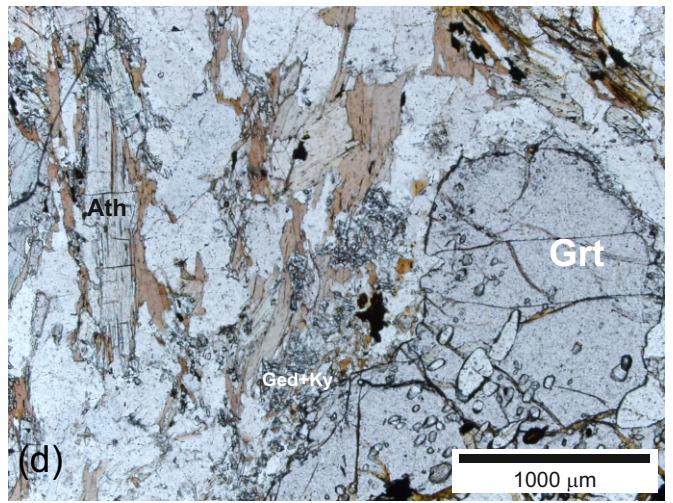
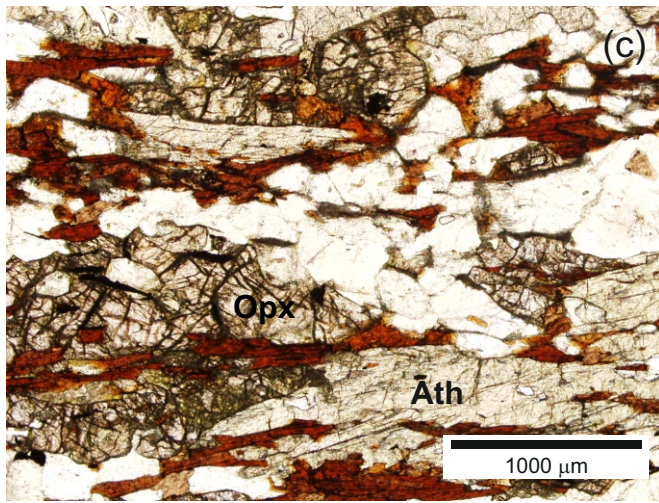
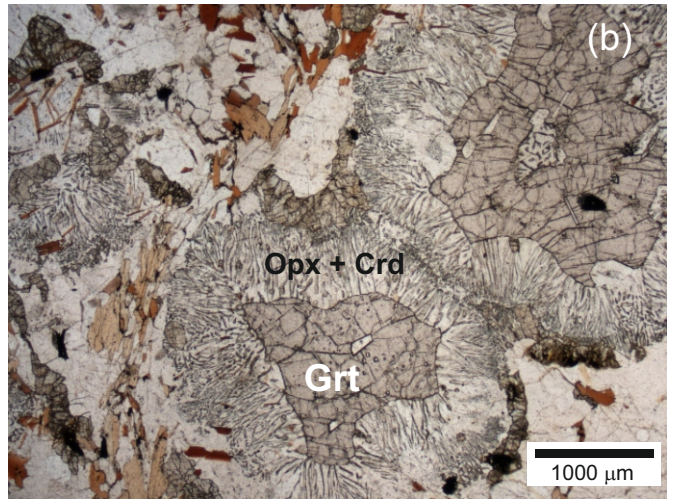
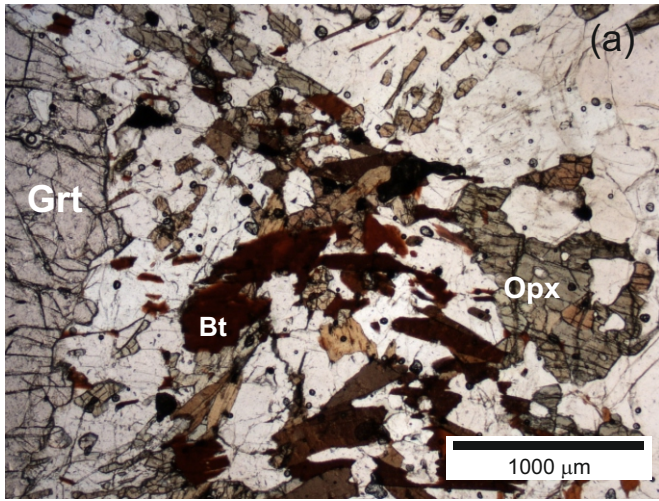


Figure 6 (colour)

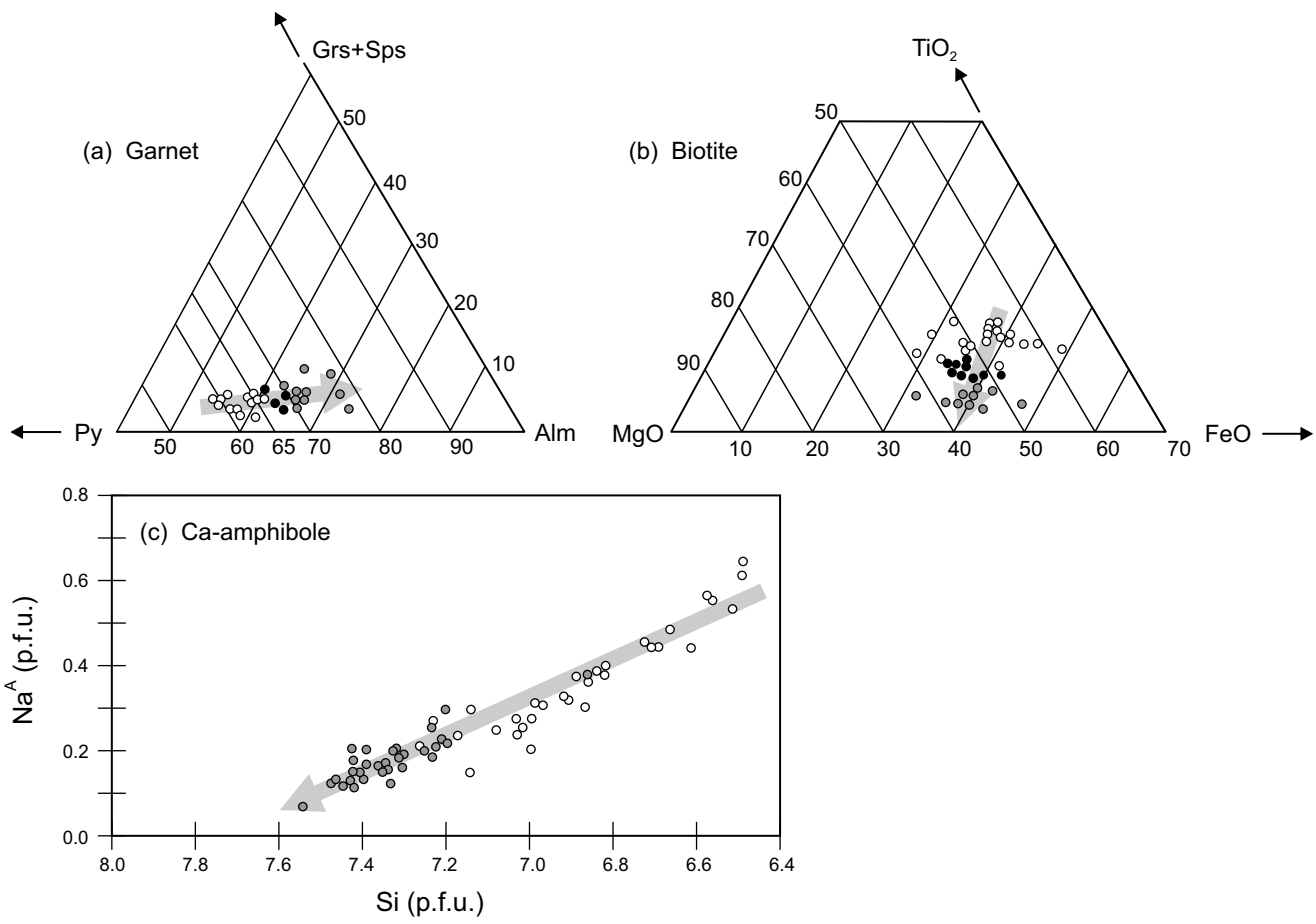


Figure 7

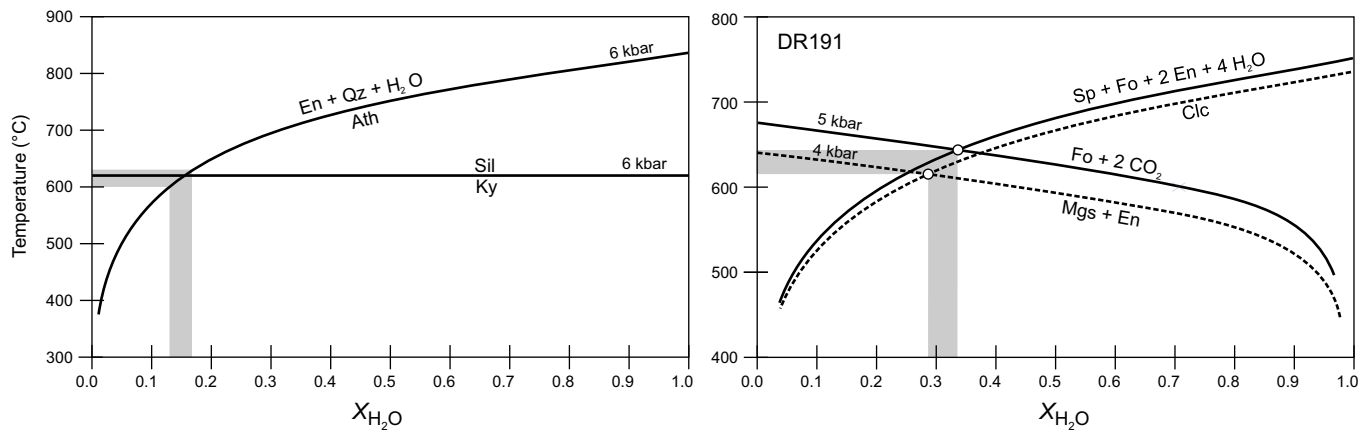


Figure 8

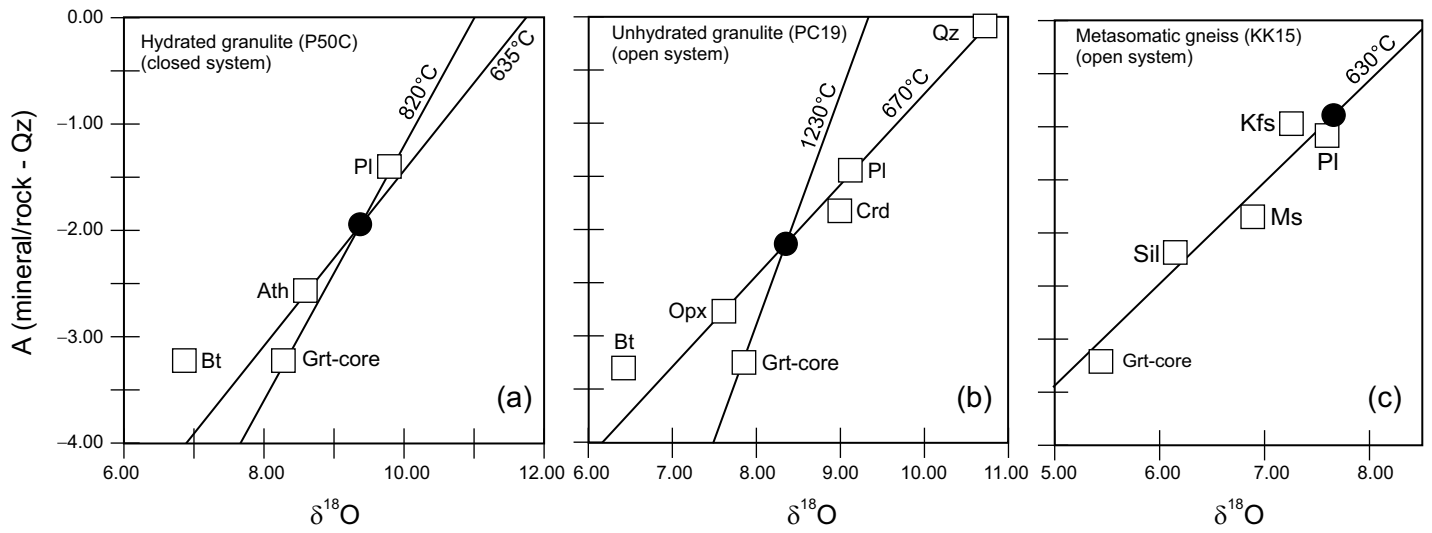


Figure 9



Figure 10 (colour)

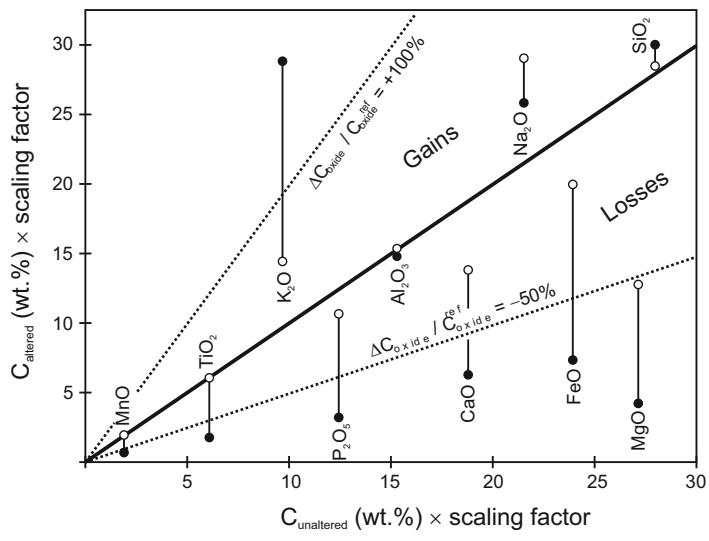


Figure 11

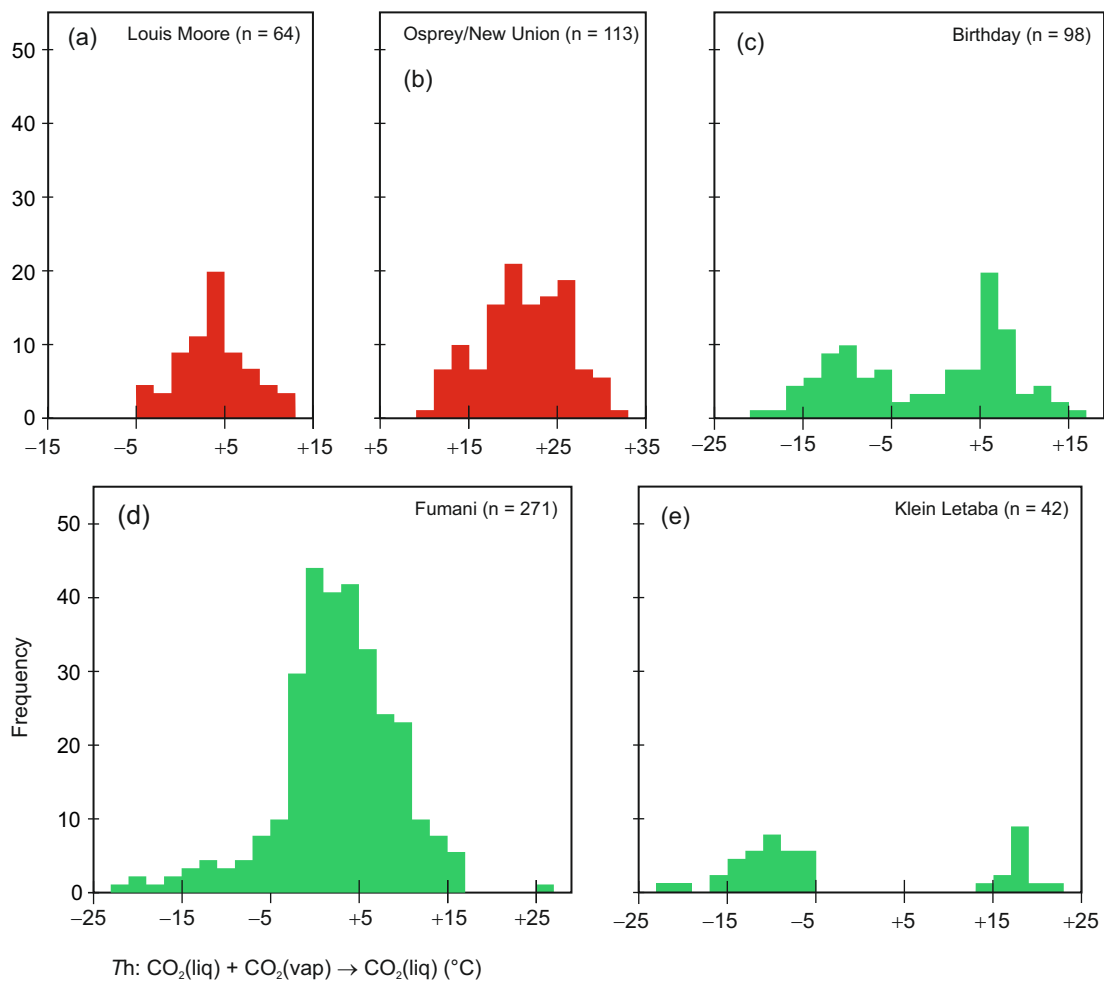


Figure 12 (colour)

Table 1

Deposit and age	Structure and metamorphism	Ore body and Au mineralization	Wall-rock alteration
Birthday (> 2.43 Ga)	SW-verging lower-amphibolite facies thrust shear zone in amphibolite schists	Hbl-Bt-Pl-Cc-Qz schist. Au (free milling) occurs in Qz veins and silicate minerals	Bt, Cc, sulphides
Fumani (> 2.63 Ga)	SW-verging upper-amphibolite facies thrust shear zone (HRSZ) in (ultra) mafic schists and BIF	Ca-Grt+Gru+Bt+Pl+Cc+Qtz schist. Au occurs as inclusions in Apy, Po, and as free milling in Qz veins and silicate minerals	Bt, Cc, sulphides
Klein Letaba (> 2.66 Ga)	SW-verging upper-amphibolite facies thrust shear zone (HRSZ) in (ultra) mafic schists, metapelites and BIF	Hbl-Bt-Qz schist. Au occurs as inclusions in Apy, Po and Lo, and as free milling in Qz veins and silicate minerals	Bt, Cc, sulphides
Frankie (> 2.43 Ga)	SW-verging middle-amphibolite facies thrust shear zone (HRSZ) in (ultra) mafic schists and BIF	Mag-Grt-Bt-Pl gneiss. Au occurs as inclusions in Apy, Po and Lo, and as free milling in Qz veins and silicate minerals	Bt, Cc, sulphides
Osprey, no age data available	SW-verging upper-amphibolite facies thrust shear zone in retrograde hydrated mafic and pelitic granulites, and BIF	Grt-Hbl-Qz-Pl±Cc gneiss and BIF. Au occurs as free milling in Qz veins and silicate minerals	Bt, Cc, Kfs sulphides
Louis Moore (> 2.5 Ga)	SW-verging upper-amphibolite facies thrust shear zone in partially retrograde hydrated ultramafic granulites	Ol-Opx-Chl-Bt-Cc schist. Au (free milling) occurs in Qz veins and silicate minerals	Bt, Cc, sulphides
Doornhoek (> 2.4 Ga)	Upper-amphibolite facies strike slip shear zone in partially retrograde hydrated ultramafic and metapelitic granulites, and BIF	Qz veins associated with sheared BIF. Au occurs as inclusions in Apy, Po and Lo, and as free milling in Qz veins and silicate minerals	Bt, Cc, Kfs sulphides